#### DOI: 10.1111/bph.70121

#### RESEARCH ARTICLE



# Structure-activity relationship of the allosteric effects of ivermectin at human P2X4 and GABA<sub>A</sub> receptors

Jessica L. Meades 1 | Marcella Bassetto 2,3 | Marius C. Staiculescu 4 | Gayathri Swaminath 4 | Samuel J. Fountain 1 0

#### Correspondence

Samuel J. Fountain, School of Biological Sciences, University of East Anglia, Norwich Research Park, Norwich, UK. Email: s.j.fountain@uea.ac.uk

### **Funding information**

This work was funded by the British Heart Foundation (PG/16/69/32194) and a Biotechnology and Biological Sciences iCASE award with Merck Sharp & Dohme LLC, a subsidiary of Merck & Co., Inc., Rahway, NJ, USA.

#### **Abstract**

Background and purpose: Positive allosteric modulation of the P2X4 receptor is a potential route to providing cardiovascular benefit through enhancing flow-dependent arterial vasodilation and providing cardioprotection. However, ligands that selectively enhance P2X4 activity are absent. The broad-spectrum antiparasitic ivermectin (MK-933) is a known positive allosteric modulator of P2X4, but not selective for P2X4, acting to enhance the activity of other ion channels including the GABA<sub>A</sub> receptor through which its neurotoxic and anti-convulsant properties are mediated. Here, we combine complementary methodology to investigate the structure-activity relationship of ivermectin at human P2X4 and GABA<sub>A</sub> receptors.

Experimental approach and key results: Intracellular  $Ca^{2+}$  and membrane potential assays in cell lines expressing human P2X4 or human GABA<sub>A</sub>  $\alpha 1\beta 3\gamma 2$  receptor are used, respectively. A chemical library of ivermectin analogues are pharmacologically characterised at both receptors, and in silico techniques are used to identify ligand binding modes in human P2X4 to interpret pharmacological properties. We identify ivermectin-B1a as a positive allosteric modulation of P2X4, but full agonist at the GABA<sub>A</sub>  $\alpha 1\beta 3\gamma 2$  receptor. We discover that the large disaccharide moiety of ivermectin-B1a is not required for activity. We identify an intersubunit transmembrane domain binding mode for ivermectin-B1a in P2X4 supported by the structure-activity relationship of ivermectin analogues. A series of novel compounds with selectivity for P2X4 over GABA<sub>A</sub> receptor are identified.

Conclusions and implications: Ivermectin-B1a enhances P2X4 and GABA<sub>A</sub>  $\alpha 1\beta 3\gamma 2$  receptor activity but through differing pharmacological mechanisms. We identify pharmacophore information for the development of positive allosteric modulators selective for human P2X4 over GABA<sub>A</sub> receptors.

#### KEYWORDS

allosteric, GABA, ion channel, P2X, purinergic

Abbreviations: PAMs, positive allosteric modulator; SAR, structure-activity relationship; SBS, salt-buffered saline.

This is an open access article under the terms of the Creative Commons Attribution License, which permits use, distribution and reproduction in any medium, provided the original work is properly cited.

© 2025 The Author(s). British Journal of Pharmacology published by John Wiley & Sons Ltd on behalf of British Pharmacological Society.

<sup>&</sup>lt;sup>1</sup>School of Biological Sciences, University of East Anglia, Norwich Research Park, Norwich, UK

<sup>&</sup>lt;sup>2</sup>School of Pharmacy and Pharmaceutical Sciences, Cardiff University, Cardiff, UK

<sup>&</sup>lt;sup>3</sup>Department of Chemistry, Faculty of Science and Engineering, Swansea University, Swansea. UK

<sup>&</sup>lt;sup>4</sup>Merck & Co., Inc., South San Francisco, California, USA

#### 1 | INTRODUCTION

Ivermectin (MK-933) belongs to a class of macrocyclic lactones with broad-spectrum antiparasitic properties in humans, companion animals and livestock, and is derived from avermectin, a natural product of the bacterium Streptomyces avermectinius (Campbell, 2012). In invertebrate parasites such as nematodes, ivermectin disrupts neuromuscular transmission through activation of pentameric glutamategated chloride channels causing muscle hyperpolarisation and paralysis (Wolstenholme & Rogers, 2005). Although ivermectin is generally considered a safe antiparasitic drug, a number of reports of severe toxic neurological side effects in humans and animals including dizziness, depression and coma have been linked to accidental overdose or when the blood-brain barrier is compromised, specifically through the dysfunction or absence of P-glycoproteins (Chandler, 2018; Edwards, 2003; Ménez et al., 2012). Invertebrate pentameric glutamate-gated chloride channels share structure similarities with mammalian cys-loop receptors. Ivermectin is known to facilitate the activity of a number of mammalian cys-loop receptors including the GABA receptor (Adelsberger et al., 2000), glycine receptors (Shan et al., 2001) and the α7 nicotinic acetylcholine receptor (Burke et al., 2024). Enhancement of GABA<sub>A</sub> receptor activity is suggested to underlie many of the neurotoxic and anti-convulsant properties of the avermectins (Coccini et al., 1993; Dawson et al., 2000; Krůšek & Zemková, 1994; Spampanato et al., 2018).

The activity of the P2X4 receptor for extracellular ATP is also facilitated by ivermectin (Fountain & North, 2006), though they are trimeric receptors and not structurally related to cys-loop receptors. Ivermectin has become a useful experimental pharmacological tool when investigating the role of P2X4 in ATP-mediated responses (Layhadi et al., 2018; Layhadi & Fountain, 2019). Earlier work by Priel and Silberberg (2004) revealed that ivermectin facilitates P2X4 receptor activity by increasing current amplitude, reducing channel desensitisation and slowing channel deactivation through stabilisation of the open channel state. P2X receptor subtypes (P2X1-7) have highly conserved orthosteric binding sites for ATP that reside at the interface between neighbouring subunits of the P2X trimer (Hattori & Gouaux, 2012), limiting the options for design of subtype-specific allosteric modulates targeting the ATP binding site. Allosteric sites within P2X receptors therefore provide an opportunity for receptor subtypespecific pharmacological regulation (Bidula et al., 2022). Ivermectin binds within the transmembrane domains of the nematode glutamateactivated chloride channel, stabilising the open channel conformation (Hibbs & Gouaux, 2011). Similarly, numerous mutagenesis studies have identified the importance of transmembrane domains within the P2X4 receptor in mediating the effects of ivermectin (Samways et al., 2012; Silberberg et al., 2007; Tvrdonova et al., 2014), and a transmembrane binding site for ivermectin has been predicted for rat P2X4 (Pasqualetto et al., 2018). However, more recent studies have proposed an ivermectin binding pocket in the extracellular domain of the P2X4 receptor (Weinhausen et al., 2022). The P2X4 receptor

#### What is already known?

 Ivermectin is a non-selective positive allosteric modulator of the P2X4 receptor

#### What does this study add?

 The chemical space influencing ivermectin potency and efficacy at P2X4 and selectivity over GABAA receptors

#### What is the clinical significance?

Selective P2X4 positive allosteric modulators are potentially useful as vasodilators

plays important roles in the central nervous system and cardiovascular system. In the central nervous system, P2X4 plays a role in synaptic plasticity in the mesocorticolimbic pathway (Rubio & Soto, 2001) and alcohol use disorder (Franklin et al., 2014). P2X4 activity in the spinal microglial is also important for the onset of neuropathic pain (Tsuda et al., 2003). The predominant physiological role identified for P2X4 is within the cardiovascular system including the control of arterial tone, where the shear stress of luminal fluid flow causes vasodilation dependent upon endothelial P2X4 receptors (Yamamoto et al., 2000; Yamamoto et al., 2006). The mean arterial blood pressure of P2X4 knockout mice is elevated and limited flow-dependent vascular remodelling is observed compared to wild-type littermates (Yamamoto et al., 2006). In humans, a loss of function polymorphism is associated with increased pulse pressure (Stokes et al., 2011). It has also been demonstrated that the P2X4 receptor serves a protective role in experimental models of heart failure and ischaemic stroke (Ozaki et al., 2016; Yang et al., 2014; Yang et al., 2015). Such studies suggest that beyond their use as experimental tools, positive allosteric modulators (PAMs) of P2X4 could have cardiovascular benefit. Despite recent advances in the clinical development of P2X receptormodulating drugs (Richards et al., 2019) and in selective antagonists of P2X4 (Stokes et al., 2017), selective PAMs of the P2X4 receptor do not currently exist.

This study sought to explore the relationship between the structure and pharmacological activity of ivermectin using a series of chemical analogues at human P2X4 and  $\mathsf{GABA}_\mathsf{A}$  receptors and using molecular modelling in an effort to identify chemical and molecular determinants of ivermectin potency, maximal level of potentiation and selectivity as an allosteric modulator.

#### 2 | METHODS

### 2.1 | Ivermectin analogues

Commercially available compounds were purchased as follows: ivermectin, doramectin, eprinomectin and moxidectin (Life Sciences, Merck & Co., Inc., Rahway, NJ, USA); ivermectin-B1a, ivermectin-B1b, abamectin, selamectin, milbemectin and nemadectin (Cayman Chemical, Cambridge, UK). A series of ivermectin analogues were provided collaboratively by Merck & Co., Inc., Rahway, NJ, USA. The chemical structures of all the ivermectin analogues investigated in this study are given in Figure S1.

#### 2.2 | Cell lines and culture

A 1321N1 cell line (RRID:CVCL\_0110) stably expressing the human P2X4 receptor has been described previously (Ahmad Nadzirin et al., 2021). A mouse L (tk-) fibroblast cell line (RRID:CVCL\_4536) expressing the human  $\alpha1\beta3\gamma2$  GABAA receptor was provided collaboratively by collaboratively by Merck & Co., Inc., Rahway, NJ, USA, and described previously (Atack et al., 2009; Atack et al., 2011). All cells were maintained in Dulbecco's Modified Eagle Medium containing 10% (v/v) fetal bovine serum, 2-mM L-glutamine, 50-U·ml $^{-1}$  penicillin and 50-µg·ml $^{-1}$  streptomycin. L (tk-) GABAA cells were grown in the presence of 1-mg·ml $^{-1}$  G418, and GABAA receptor expression was induced by treatment with 1-µM dexamethasone for 24 h prior to seeded for experimentation. All cells were cultured at 37°C with 5% CO $_2$  in a humidified incubator.

# 2.3 | Intracellular Ca<sup>2+</sup> assays

Assays were performed in salt-buffered saline (SBS) containing (mM): NaCl, 130; KCl, 5; MgCl<sub>2</sub>, 1.2; CaCl<sub>2</sub>, 1.5; D-glucose, 8; HEPES, 10; pH 7.4 with NaOH. 1321N1 cells were seeded at 25,000 cells per well in clear-bottomed 96-well plates. Cells were cultured overnight following the replacement of the culture medium with SBS containing 0.01% (w/v) pluronic acid and 2- $\mu$ M Fura-2AM (Abcam, Cambridge, UK). Cells were loaded with Fura-2 for 1 h at 37°C. Following loading, SBS was removed and replaced with 0.2-ml SBS. Fura-2 was excited at 340 and 380 nm, and emission at 520 nm was collected using a Flexstation 3 instrument (Molecular Devices, Wokingham, UK) and 2-s sampling. *F* ratio was calculated as 520 nm at 340/380 nm. Cells were incubated with test compounds for 20 min before ATP application unless otherwise stated. All experiments were performed at 37°C. The peak Ca<sup>2+</sup> response is represented in concentration-response curves and used for statistical comparison throughout.

# 2.4 | Membrane potential measurements

A fluorescent membrane potential dye FMP-Red dye (Molecular Devices) was used to quantitate GABA<sub>A</sub> receptor activity as previously described (Joesch et al., 2008). L (tk-) GABA<sub>A</sub> cells were seeded

at 35,000 cells per well in clear bottom 96-well plates 24 h before experimentation. Culture medium was removed and replaced with assay buffer containing (mM): CaCl<sub>2</sub>, 1.3; MgCl<sub>2</sub>, 0.5; MgSO<sub>4</sub>, 0.4; KCl, 5.3; KH<sub>2</sub>PO<sub>4</sub>, 0.4; NaHCO<sub>3</sub>, 4.2; NaCl, 138; Na<sub>2</sub>HPO<sub>4</sub>, 0.3; D-glucose 5.6; HEPES, 4.7; pH 7.4 with NaOH. The assay contained  $1\times$  FMP-Red-Dye as instructed by the supplier. Cells were incubated with dye for 1 h at 37°C prior to experimentation. A Flexstation 3 instrument was used to excite the dye at 530 nm and measure emission at 565 nm. Emission was sampled every 5 s for 300 s. All experiments were performed at 37°C. Control wells were injected with assay buffer alone and an averaged respond was subtracted from all experimental values to control for injection artefacts.

# 2.5 | Experimental design and statistical analysis

Experimental design, analysis and disclosure follow the guidance outlined by Curtis et al. (2025). Data are expressed as mean  $\pm$  SE, and n is the number of independent biological experiments, with data values for independent experiments derived from the average of three technical repeats within an assay. Statistical analysis was performed using independent values from technical repeats using OriginPro software (v2019; OriginLab). A threshold for statistical analysis of P < 0.05 was applied throughout. Data normality was assessed using a Shapiro–Wilk test and Levene's test for equality of variance. Normally distributed data were assessed using an unpaired two-sample t-test or a one-way ANOVA followed by a post hoc Tukey test. Post-hoc tests were run only if F achieved P<0.05 and there was no significant variance inhomogeneity. A Mann–Whitney test or a Kruskal–Wallis ANOVA followed by post hoc analysis was used for data that were not normally distributed.

Concentration-response curves were fitted using a modified Hill equation:

$$Y = Start + (End - Start) \frac{X^n}{k^n + X^n}$$

where K is the Michaelis constant and n is the number of cooperative sites. Concentration values for ligand effects are reported as logarithmic means throughout.

# 2.6 | Blinding

Experimenters were blinded to the chemical structures of test compounds when performing activity analysis at P2X4 and GABA<sub>A</sub> receptors. Experimenters were blinded to the activity of compounds when performing in silico binding mode analysis.

### 2.7 | Molecular modelling

All molecular modelling experiments were performed on an Asus WS X299 PRO Intel  $^{@}$  i9-10980XE CPU @ 3.00GHz  $\times$  36 running Ubuntu 18.04 (graphic card: GeForce RTX 2080 Ti). Molecular Operating

Environment (MOE, 2022.02, Montreal, QC, Canada) and Maestro (Schrödinger Release 2024-2, New York, NY, USA) were used as molecular modelling software. A homology model for the human P2X4 receptor (Uniprot ID Q99571, https://www.uniprot.org/) in the open, ATP-bound state was built from the crystal structure of the openconformation zebrafish receptor (PDB ID 4DW1, http://www.rcsb. org/), using a single-template approach in MOE 2022.02. Sequence alignment between the human and zebrafish sequences was performed using Clustal Omega (Sievers et al., 2011). MOE SiteFinder tool was used to locate predicted druggable sites on the model, between the first and second transmembrane domain, as previously described by Pasqualetto et al. (2018), and in correspondence of an alternative site in the extracellular domain recently described by Weinhausen et al. (2022). The model was saved in the mae format and preprocessed using Schrödinger Protein Preparation Wizard, by assigning bond orders, adding hydrogens and performing a restrained energy minimisation of the added hydrogens using the OPLS 2005 force field. Two 15-Å docking grids were prepared, using as centroid the coordinates of the central alpha sphere of each site identified by MOE SiteFinder. The structures of ivermectin-B1a and a representative selection of its analogues were built in MOE, saved in the sdf format and prepared using the Maestro LigPrep tool by energy minimising the structures (OPLS 2005 force filed), generating possible ionisation states at pH 7 ± 2 (Epik), generating tautomers and low-energy ring conformers. The ligands were analysed for their predicted binding to the two potential sites of the model using the Glide SP docking algorithm, using the default parameters. Twenty-five output poses for each ligand were visually inspected to evaluate common binding modes for each site. In this evaluation, a docking pose was considered as favourable when associated to a low docking score, relative to those observed for the compounds analysed and the two different sites explored, to the ability of any given compound to occupy a well-defined portion of space and to the ability of any given compound to make nonbonded interactions with the amino acid residues defining each binding pocket. A table with the Glide SP docking score values for the compounds evaluated is provided in Table S1. The ivermectin-B1a-P2X4 binding model PBD file is available upon reasonable request to the corresponding author.

#### 2.8 | Nomenclature of targets and ligands

Key protein targets and ligands in this article are hyperlinked to corresponding entries in the IUPHAR/BPS Guide to PHARMACOLOGY <a href="http://www.guidetopharmacology.org">http://www.guidetopharmacology.org</a> and are permanently archived in the Concise Guide to PHARMACOLOGY 2023/23 (Alexander, Fabbro, et al., 2023; Alexander, Mathie, et al., 2023).

#### 3 | RESULTS

# 3.1 | Ivermectin effects and predicted binding site

ATP evoked concentration-dependent intracellular Ca<sup>2+</sup> responses in 1321N1 cells stably expressing human P2X4 receptors (Figure 1a)

with pEC<sub>50</sub> and pEC<sub>30</sub> values of  $6.30 \pm 0.05$  (n = 5) and  $6.52 \pm 0.08$ (n = 5), respectively (Figure 1b). ATP-evoked responses were not observed in untransfected 1321N1 cells (Figure 1c), though activation of endogenous muscarinic receptors with carbachol was evident (Figure 1c). An approximate pEC<sub>30</sub> value of 6.52 for ATP was selected in later studies to investigate the effects of PAMs. Most studies employing ivermectin as a P2X4 modulator use a commercially available form consisting of a mix of major homologues ivermectin-B1a and ivermectin-B1b in a 19:1 M ratio, which is referred to as ivermectin throughout. Ivermectin potentiated ATP-evoked Ca<sup>2+</sup> responses with an pEC<sub>50</sub> of  $6.10 \pm 0.06$  (n = 5) (Figure 1d), increasing the maximal response to ATP by 556 ± 46%. Ivermectin did not directly activate human P2X4 (data not shown). Ivermectin-B1a and ivermectin-B1b potentiated ATP-evoked Ca<sup>2+</sup> responses (Figure 1f) with pEC<sub>50</sub> values of  $6.00 \pm 0.08$  (n = 5) and  $6.03 \pm 0.05$  (n = 5), respectively (Figure 1g). The potencies of ivermectin-B1a and ivermectin-B1b were not significantly different to that of ivermectin or each other (P > 0.05) (Table 1). However, the maximal level of potentiation by both ivermectin-B1a and ivermectin-B1b was significantly less than by ivermectin (P < 0.05), potentiating by  $391 \pm 40\%$ (n = 5) and 356 ± 51% (n = 5), respectively (Table 1). As ivermectin is a mixture of two distinct chemical entities, we used ivermectin-B1a as a reference point for comparing the activity of other ivermectin homologues.

We used a homology model of the human P2X4 receptor in the open state to predict binding sites for ivermectin-B1a and a selection of analogues tested, in an effort to further understand how differing chemistry impacts on potentiator activity. With the aim of providing a rationale to the observed structure-activity relationship (SAR) for ivermectin-B1a analogues, we explored the two previously reported. putative binding sites for ivermectin-B1a, one between receptor transmembrane domains, previously described by Pasqualetto et al. (2018), and an alternative extracellular binding site, more recently described by Weinhausen et al. (2022) (Figure 2a). A molecular docking analysis was performed for ivermectin-B1a and its analogues to both sites, as defined using the SiteFinder tool in MOE 2022.02. The SAR data of the analogue experimental evaluation were used as a framework to help assess the likelihood of the binding modes observed. Our final predicted binding mode for ivermectin-B1a and its analogues was identified with a combined evaluation of the docking score for each generated pose, and the number of times the same or a very similar pose is repeated within the best 25 low-energy poses produced by the docking algorithm and visually inspected for each compound. A binding mode for ivermectin-B1a consistent with the structure-activity information was identified within the transmembrane domains, in proximity to Trp46, Asp331 and Met336 and consistent with Franklin et al. (2014). No binding modes in line with the structure-activity information for ivermectin-B1a or its analogues tested could be identified in the allosteric site proposed by Weinhausen et al. (2022). Ivermectin is a macrocyclic lactone containing a core central 16-carbon macrocyclic ring and three distinct chemical moieties including disaccharide, spiroketal and benzofuran moieties (Figure 2b). Our model reveals an intersubunit binding pocket for ivermectin-B1a (Figure 2c). The spiroketal group extends between

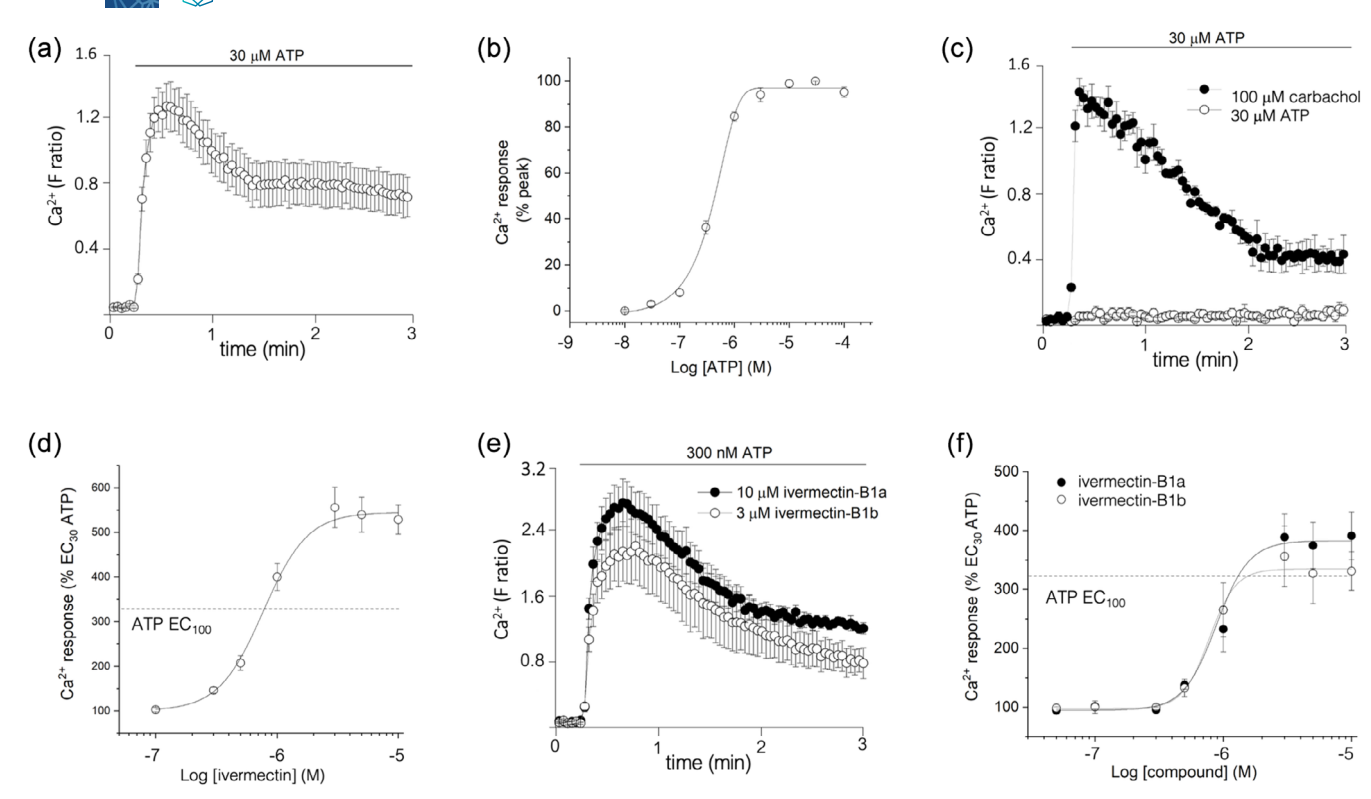


**FIGURE 1** Effect of ivermectin, ivermectin-B1a and ivermectin-B1b on human P2X4 receptor responses. (a) Average trace showing ATP-evoked  $Ca^{2+}$  response in 1321N1 human P2X4 cells (n=8). Magnitude of response expressed as Fura-2 F ratio (b) ATP concentration-response in 1321N1 human P2X4 cells (n=5). Response expressed as % maximum. (c)  $Ca^{2+}$  response evoked by carbachol but not by ATP in untransfected 1321N1 cells (n=5). Magnitude of response expressed as Fura-2 F ratio. (d) Concentration-response curve showing ivermectin potentiation of ATP-evoked  $Ca^{2+}$  responses in 1321N1 human P2X4 cells (n=5). (e) Potentiation of ATP-evoked  $Ca^{2+}$  responses by ivermectin-B1a or ivermectin-B1b in 1321N1 human P2X4 cells (n=5). Magnitude of response expressed as Fura-2 F ratio. (f) Concentration-response curve showing ivermectin-B1b potentiation of ATP-evoked  $Ca^{2+}$  responses in 1321N1 human P2X4 cells (n=5). Dotted lines in concentration-response curves marked ATP  $EC_{100}$  illustrate the maximum response to ATP without test ligand.

transmembrane domains, occupying the space defined by sidechains of Trp46 and Ile333 of one transmembrane domain, and the sec-butyl substituent occupying a small, recessed area defined by the sidechains of Asp331, Pro334 and Glu56 of the adjacent subunit (Figure 2c). We have defined Subsite 1 with an upper part comprising sidechains of Trp46, Glu51 and Ile333 interacting with the majority of the spiroketal group and a lower part comprising sidechains of Tyr42 and Ile337 interacting with the majority of the benzofuran group (Figure 2a). We also defined Subsite 2 (Asp331, Ile333, Pro334, Glu56) that binds the sec-butyl substituent of the spiroketal group. Direct contacts are predicted between the sidechain of Glu51 and Trp46 and both furan and spiroketal rings (Figure 2c). Interestingly, this binding pose predicts that the disaccharide group points towards the central cavity defined by the three receptor subunits, making only one nonbonded interaction between the methoxy oxygen atom of the central sugar unit and the sidechain of Lys197 and exposed towards the solvent-accessible area. The disaccharide group is therefore almost entirely solventexposed (Figure 2d). An expanded version on the ivermectin binding mode is given in Figure S2.

The compounds investigated in this study contained chemical substituents in disaccharide, spiroketal and benzofuran moieties, allowing interrogation of the predicted ivermectin-B1a binding site and an understanding of the structure–activity relationship of the compounds tested. The structures of all compounds tested are given in Figure S1. For all compounds tested, no direct agonist activity at P2X4 was observed up to a maximal concentration of 30  $\mu$ M tested. A set of key ligand–receptor interactions are given in 2D in Figure S3.

# 3.2 | Compounds with modification to the disaccharide group

Milbemectin is chemically identical to ivermectin-B1a except it lacks the disaccharide group. Despite this, milbemectin potentiated P2X4 responses (Figure 3a) with similar potency and maximal level of potentiation as ivermectin-B1a (Figure 3b) (Table 1). Milbemectin was predicted to make the same contacts as ivermectin-B1a spiroketal and benzofuran groups (Figure 3c). These data suggest that the disaccharide group is not required for compound action despite being a substantial part of the molecule. These functional data support the lack of significant interaction between the receptor and the disaccharide group in the predicted binding mode (Figure 2). Chemical modifications within the disaccharide group at Carbon 4" were

TABLE 1 Effect of ivermectin analogues on human P2X4 responses ranked by potentiator effect

Compound	pEC <sub>50</sub> <sup>a</sup>	Hill slope	Response (% vehicle control) <sup>b</sup>	Potentiation (% ivermectin-B1a)	Site(s) of chemical modification
Abamectin	6.45 ± 0.06*	1.7 ± 0.1	967.47 ± 65.76*	247.40	Spiroketal
Nemadectin	6.46 ± 0.06*	2.9 ± 0.3	803.40 ± 65.76*	205.44	Disaccharide, spiroketal
Compound 25	5.50 ± 0.04*	2.9 ± 0.4	642.62 ± 25.87*	164.33	Spiroketal
Doramectin	6.42 ± 0.05*	3.1 ± 0.1	641.01 ± 32.34*	163.92	Spiroketal
Compound 19	5.94 ± 0.10	2.2 ± 0.5	578.92 ± 66.85*	148.04	Spiroketal
Ivermectin	6.13 ± 0.01	2.9 ± 0.5	555.90 ± 45.51*	142.15	Spiroketal
Compound 26	5.62 ± 0.03*	2.4 ± 0.6	549.40 ± 37.13*	140.52	Disaccharide
Compound 1	5.62 ± 0.01	2.6 ± 0.1	511.53 ± 65.10	130.81	Spiroketal
Moxidectin	6.29 ± 0.01*	1.8 ± 0.2	491.91 ± 25.36	126.56	Disaccharide, spiroketal
Eprinomectin	6.02 ± 0.07	2.3 ± 0.3	472.63 ± 27.86	120.86	Disaccharide, spiroketal
Milbemectin	6.10 ± 0.03	2.1 ± 0.5	448.38 ± 48.22	114.66	Disaccharide
Compound 8	6.00 ± 0.09	2.2 ± 0.3	424.54 ± 89.50	108.56	Benzofuran
Selamectin	6.20 ± 0.08	1.8 ± 0.2	423.29 ± 28.08	108.24	Benzofuran, disaccharide, spiroket
Compound 27	6.24 ± 0.04	2.8 ± 0.4	409.73 ± 34.03	104.77	Benzofuran
Ivermectin-B1a	5.99 ± 0.05	3.4 ± 0.5	391.06 ± 40.37	100.00	-
Compound 14	6.23 ± 0.18	3.7 ± 0.3	390.67 ± 23.80	99.90	Spiroketal
Compound 22	6.16 ± 0.07*	4.1 ± 0.3	390.05 ± 30.21	99.74	Benzofuran
Ivermectin-B1b	6.12 ± 0.06	4.2 ± 0.5	356.19 ± 51.52	91.08	Spiroketal
Compound 2	6.03 ± 0.05	2.7 ± 0.2	354.65 ± 44.23	90.89	Disaccharide
Compound 4	6.07 ± 0.08	3.9 ± 0.1	337.40 ± 8.66	86.28	Benzofuran
Compound 24	5.76 ± 0.02	2.9 ± 0.2	321.94 ± 52.22	82.33	Benzofuran
Compound 10	6.01 ± 0.09	2.3 ± 0.2	285.85 ± 22.69	73.10	Benzofuran, disaccharide
Compound 13	5.65 ± 0.06*	2.8 ± 0.4	269.46 ± 20.84	68.91	Spiroketal
Compound 20	5.91 ± 0.09	4.7 ± 0.6	245.8.6 ± 16.20*	62.87	Benzofuran
Compound 11	6.15 ± 0.10	0.2 ± 0.0	203.42 ± 22.69*	52.05	Disaccharide
Compound 6	6.16 ± 0.05	2.3 ± 0.2	192.38 ± 18.66*	49.19	Benzofuran
Compound 16	n.d.	n.d.	170.97 ± 3.60*	43.72	Spiroketal
Compound 12	5.52 ± 0.07*	5.4 ± 0.4	158.28 ± 16.00*	40.47	Spiroketal
Compound 9	n.d.	n.d.	136.66 ± 11.39*	35.00	Spiroketal
Compound 23	n.d.	n.d.	136.29 ± 0.60*	34.85	Spiroketal
Compound 17	n.d.	n.d.	131.79 ± 18.63*	33.70	Benzofuran, spiroketal
Compound 21	n.d.	n.d.	126.39 ± 13.54*	33.06	Spiroketal
Compound 5	n.d.	n.d.	121.14 ± 5.63*	30.89	Benzofuran, disaccharide, spiroket
Compound 18	n.d.	n.d.	118.35 ± 7.91*	30.26	Benzofuran, disaccharide
Compound 15	n.d.	n.d.	115.74 ± 11.10*	29.60	Benzofuran, spiroketal
Compound 7	n.d.	n.d.	111.34 ± 14.42*	28.47	Benzofuran, disaccharide, spiroket
Compound 3	n.d.	n.d.	109.67 ± 9.88*	28.05	Spiroketal

Note: n = 6-8 for all.

Abbreviation: n.d. denotes not determined.

generally well tolerated or enhanced the activity of the compound (Table 1). The addition of a phosphate group (Compound 2) was well tolerated (Figure 3d,e) (Table 1), whereas the addition of a methyl phosphate group (Compound 11) significantly reduced compound

maximal level of potentiation (Figure 3f,g) (Table 1). Interestingly, a succinic acid additional (Compound 26) significantly reduced potency but enhanced compound maximal level of potentiation (Figure 3h,i) (Table 1).

<sup>&</sup>lt;sup>a</sup>Determined against pEC<sub>30</sub> ATP (6.52).

 $<sup>^{\</sup>mathrm{b}}\mathrm{Determined}$  using maximum concentration of analogue against pEC  $_{30}$  ATP (6.52). % vehicle control peak response.

<sup>\*</sup>Denotes a significance level of P < 0.01 compared with ivermectin B1a.

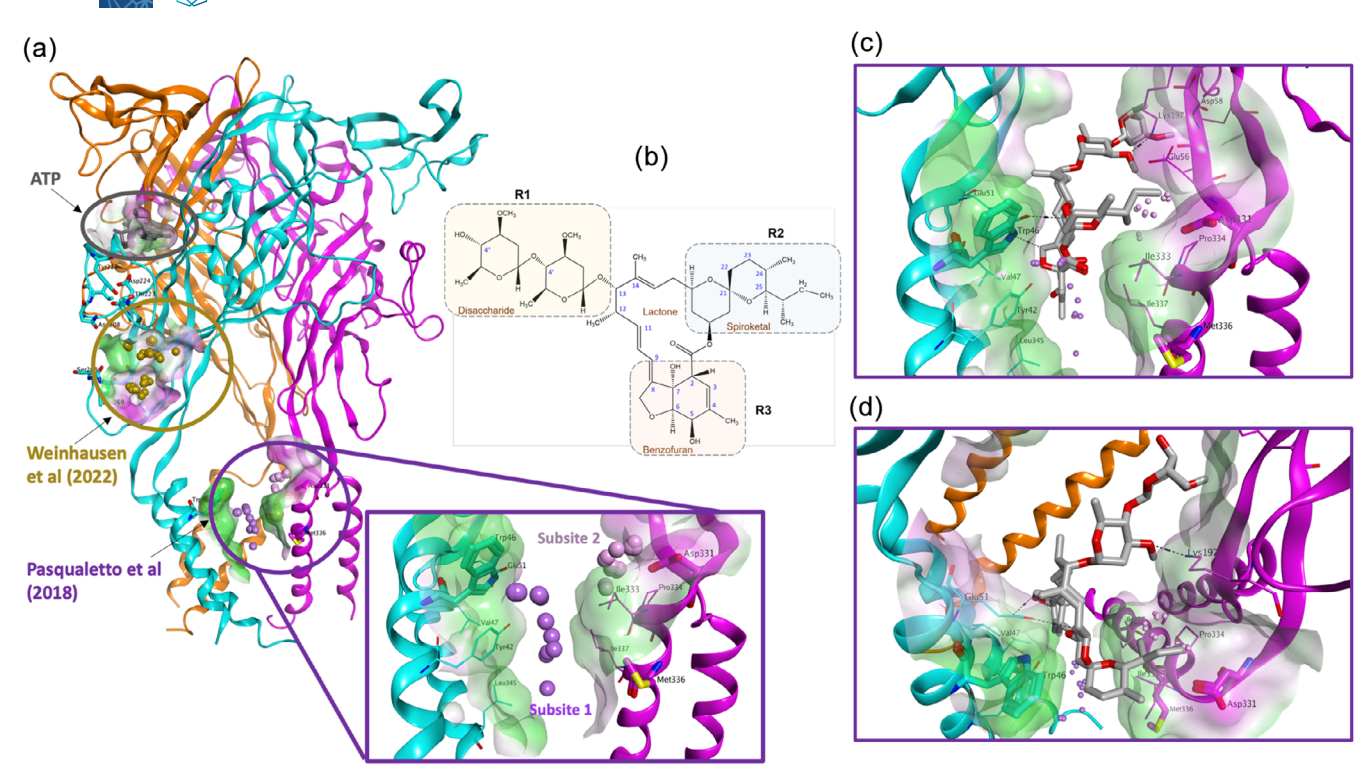


FIGURE 2 Predicted binding mode of ivermectin-B1a to the human P2X4 receptor. (a) Potential ivermectin-B1a binding sites in a homology model of P2X4 in the ATP-bound open channel conformation. The three subunits of the trimer are presented as cyan, pink and orange ribbons. The ATP binding site (grey atoms) and two putative allosteric sites predicted by Pasqualetto et al. (2018) (lilac and pink spheres) and Weinhausen et al. (2022) (ocher spheres) are shown. Surfaces are coloured green (lipophilic), white (neutral) and pink (hydrophilic). The predicted intersubunit binding pocket is shown as Subsite 1 and Subsite 2 in the expanded window. (b) Chemical structure of ivermectin-B1a showing disaccharide, lactone, spiroketal and benzofuran moieties. (c) Predicted binding mode of ivermectin-B1a and human P2X4 in the open channel conformation. Two receptor subunits defining the site are shown in cyan and pink ribbons. The available binding areas for Subsites 1 and 2 are represented as lilac and pink spheres, respectively. Residues within 4.5 Å of ivermectin-B1a are shown. (d) Top view of ivermectin-B1a predicted binding mode showing the disaccharide moiety pointing towards the central cavity defined by the three receptor subunits and almost entirely exposed to solvent.

# 3.3 | Compounds with modifications to the spiroketal group

Abamectin differs from ivermectin-B1a only by the presence of a double bond between Carbon 22-23 in the spiroketal group. Abamectin potentiated the P2X4 response approximately 2.5-fold greater than ivermectin (Figure 4a) and was more potent (Figure 4b) (Table 1). It was the compound with the highest maximal level of potentiation tested (Table 1). Doramectin, which has a carbon double bond at the same position as abamectin, in addition to a cyclohexane group at Carbon 25, also potentiated the P2X4 response beyond that of ivermectin-B1a (Figure 4c) and with greater potency (Figure 4d) (Table 1), though loss of maximal level of potentiation was observed at supramaximal concentrations (Figure 4d). The Carbon 22-23 double bond in abamectin and doramectin induces a slight rearrangement of the overall binding pose, shifting the molecules towards the central cavity (Figure 4e). The reduced flexibility associated with the unsaturation produces a more stable, simultaneous occupation of Subsites 1 and 2, potentially explaining the enhanced activity observed. The introduction of a cyclohexyl group in doramectin is predicted to enhance the spatial occupation of Subsite 2 (Figure 4f), again a

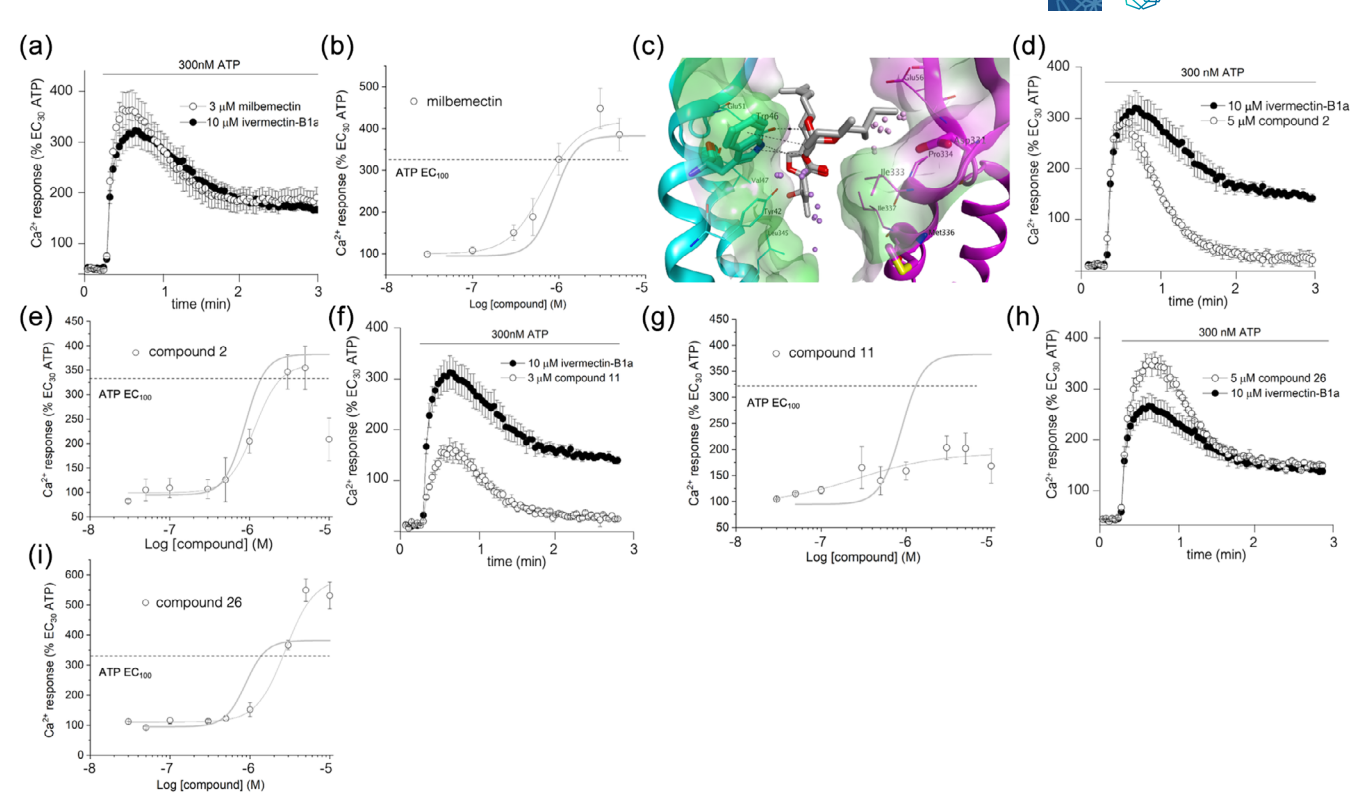
potential for enhanced activity. Some chemical additions to Carbon 23 were tolerated (Compound 1, methyl and hydroxy addition), whereas the addition of a methyl ester group (Compound 25) significantly enhanced the potentiation of P2X4 responses (Table 1). The addition of other minor chemical groups to Carbon 23 (Compounds 3, 9, 12, 16, 21 and 23) had major detrimental effects on compound activity, with compounds having little or no potentiator effects (Table 1). The insertion of a hydroxy substituent at Carbon 23 of the spiroketal group in Compound 9 is associated with a disrupted binding to Subsite 2, though the benzofuran group is still predicted to occupy Subsite 1 (Figure 4g). The introduced hydroxyl group is predicted to form a hydrogen bond with the backbone carbonyl group of Gln55, pulling the spiroketal outside the binding pocket (Figure 4g). The detrimental effect of introducing a hydroxy substituent at Carbon 23 is neutralised by the addition of a geminal methyl group as in Compound 1. The steric hinderance associated with the methyl group appears to shield the hydroxyl group and prevent hydrogen bonding with Gln55, thus restoring the binding mode (Figure 4h). No favourable docking poses were observed for Compound 16. Compounds 13 and 19 are stereoisomers of each other and of ivermectin-B1a, with one chiral centre with an enantiomeric change to the ethyl group at Carbon 25.

14765381, 2025, 21, Downloaded from https://bpspubs

onlinelibrary.wiley.com/doi/10.1111/bph.70121 by University Of East Anglia, Wiley Online Library on [08/10/2025]. See the Terms

and Condition

) on Wiley Online Library for rules of use; OA articles are governed by the applicable Creative Commons



Pharmacological properties of ivermectin analogues with a modified disaccharide moiety at human P2X4. (a) Average trace showing effect of milbemectin compared to ivermectin-B1a on ATP-evoked  $Ca^{2+}$  response in 1321N1 human P2X4 cells (n = 5). (b) Milbemectin concentration-response curve showing potentiation of ATP-evoked  $Ca^{2+}$  responses (n = 5). (c) Predicted intersubunit binding mode of milbemectin to human P2X4 in the open channel conformation. Available binding areas in Subsites 1 and 2 are represented by lilac and pink spheres, respectively. Interactions between milbemectin and receptor are shown as black dotted lines. Average trace (d) and concentrationresponse curve (e) showing effect of Compound 2 on ATP-evoked  $Ca^{2+}$  responses in 1321N1 human P2X4 cells (n = 5). Average trace (f) and concentration-response curve (g) showing effect of Compound 11 on ATP-evoked  $Ca^{2+}$  responses (n = 5). Average trace (h) and concentrationresponse curve (i) showing effect of Compound 26 on ATP-evoked  $Ca^{2+}$  responses (n = 5). The concentration-response curve to ivermectin-B1a is shown in reference as a grey curve in all test compound concentration-response curves. All Ca<sup>2+</sup> responses expressed as % response to EC<sub>30</sub> ATP. Dotted lines in concentration-response curves marked ATP EC<sub>100</sub> illustrate the maximum response to ATP without test ligand.

The enantiomeric changes lead to two largely different effects on the P2X4 response. Compound 13 potentiated P2X4 to a level not significantly different than that of ivermectin-B1a (Figure 5a), though was significantly less potent (Figure 5b) (Table 1). Compound 19 potentiated P2X4 to a greater level than ivermectin-B1a (Figure 5c) but with similar potency (Figure 5d) (Table 1). The predicted binding of the two enantiomers for the asymmetric carbon at this position, 19 (S enantiomer) and 13 (R enantiomer), is in support with Compound 19 being in the same absolute configuration as ivermectin-B1a for this asymmetric centre. The S configuration for this carbon is associated with an optimal occupation of the available space in Subsite 2, whereas the predicted binding for Compound 19 is the same as that for ivermectin-B1a (Figure 5e).

#### 3.4 Compounds with modifications to the benzofuran group

Modifications at Carbon 5 were mostly well tolerated including Compounds 8, 20 and 22 (Table 1) with the exception of a large tris(2,2,2

trichloroethyl) phosphate addition (Compound 6), which led to a significant reduction in maximal level of potentiation (Table 1). Modifications at Carbon 4 in Compounds 4, 24 and 27 were well tolerated (Table 1). This includes large 2-methoxyethoxymethyl ether and succinic acid additions as for Compounds 4 (Figure 6a,b) and 27 (Figure 6c,d), respectively. Significant loss of the maximal level of potentiation was observed for Compound 27 at supramaximal concentrations (Figure 6d). Molecular docking results predict that additions to Carbon 4 and 5 of the benzofuran group extend the occupational space towards the intracellular side of the receptor, as for Compounds 8 and 24 (Figure S2). The bulkier additional in Compound 4 also extends ligand occupation towards the intracellular side of the receptor (Figure 6e) and towards the interhelical space for Compound 27 (Figure 6f). The addition of a methoxy group at Position 5 in Compound 22 results in a significant loss of potency (Figure 6g) (Table 1) and disrupts binding, with a docking pose predicted towards the internal cavity of the receptor and associated with a significant reduction in potency (Figure 6h). Compound 20 exhibits similar potency to ivermectin but a significant reduction in the maximal level of potentiation (Figure 6i) (Table 1). The phosphate diester substituent at Carbon 5 in

**FIGURE 4** Pharmacological properties of ivermectin analogues with a modified spiroketal moiety at human P2X4. The concentration–response curve to ivermectin-B1a is shown in reference as a grey curve in all test compound concentration–response curves. (a) Average trace showing effect of abamectin compared with ivermectin-B1a on ATP-evoked  $Ca^{2+}$  response in 1321N1 human P2X4 cells (n = 5). (b) Abamectin concentration–response curve showing potentiation of ATP-evoked  $Ca^{2+}$  responses (n = 5). Average trace (c) and concentration–response curve (d) showing effect of doramectin on ATP-evoked  $Ca^{2+}$  responses (n = 5). The concentration–response curve to ivermectin-B1a is shown in reference as a grey curve in all test compound concentration–response curves. All  $Ca^{2+}$  responses expressed as % response to  $EC_{30}$  ATP. Dotted lines in concentration–response curves marked  $EC_{100}$  illustrate the maximum response to ATP without test ligand. (e-h) Front (*upper panel*) and top (*lower panel*) view of predicted binding mode of abamectin (e), doramectin (f), Compound 9 (g) and Compound 1 (h) to human P2X4 in the open channel conformation. Individual receptor subunits are represented as cyan, pink and orange ribbons. The available binding area for Subsites 1 and 2 is represented as lilac and pink spheres, respectively. The receptor binding surface is represented as green (lipophilic) and pink (hydrophilic). Relevant receptor residues are shown with carbon atoms coloured according to their ribbon, and ligand–receptor interactions represented as black dotted lines.

Compound 20 retains the spatial occupation of Subsites 1 and 2 but in an inverted fashion. The approximate 180° flip in binding confirmation leaves the disaccharide group facing the left-hand slide of the central cavity (Figure 6j). On the contrary, the removal of the carbonyl groups of the phosphate diesters in Compound 6 significantly reduces the compound maximal level of potentiation (Figure 6k) (Table 1) and disrupts binding (Figure 6l). The ligand is pushed towards the central cavity and Subsite 2 is left completely unoccupied (Figure 6l).

5294

# 3.5 | Compounds with mixed modifications

Moxidectin and nemadectin lack the disaccharide group, whereas selamectin has a monosaccharide group. Selamectin has a similar maximal level of potentiation and potency as ivermectin-B1a (Figure 7a,b) (Table 1). In keeping with this activity, the predicted binding site for selamectin reveals a retained ability to occupy Subsite 2 (Figure 7c). However, the presence of the hydroxyl-imine function at Carbon

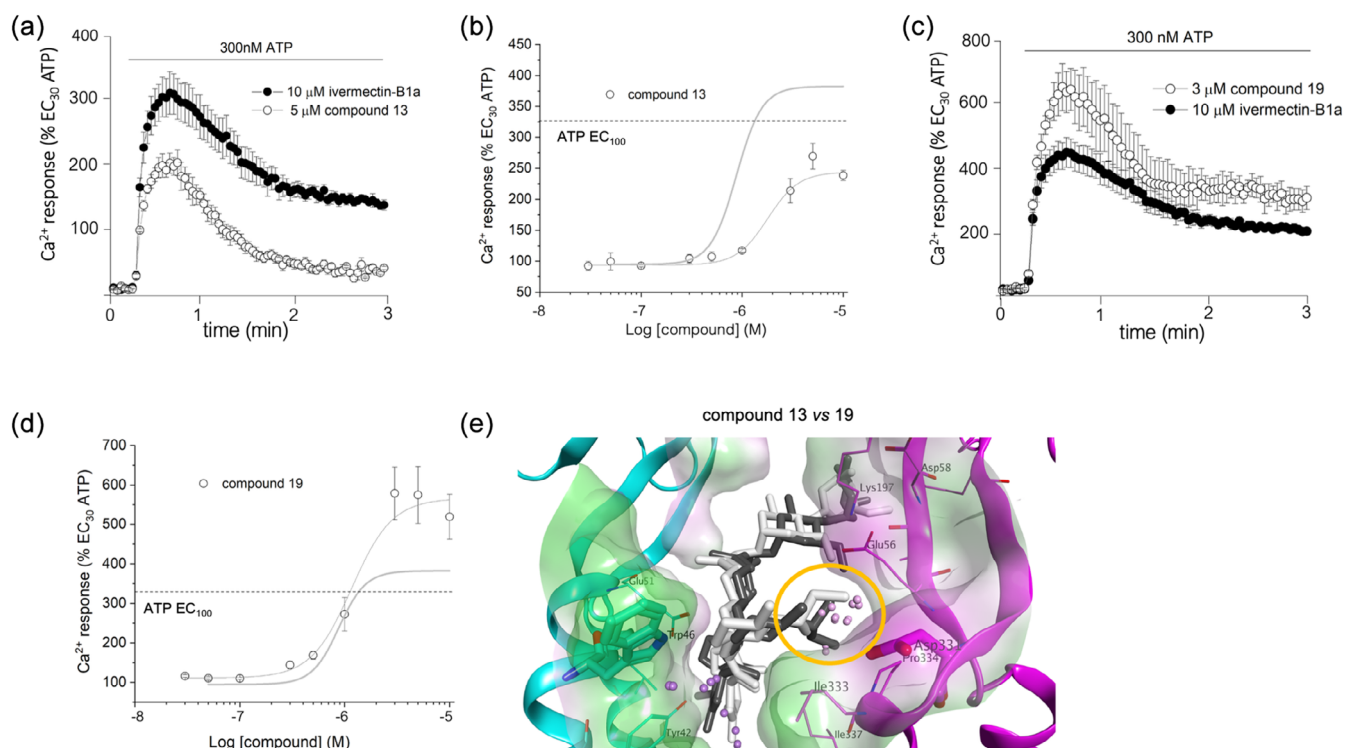
5 appears to be associated with a perturbed occupation of Subsite 1, as this group appears to pull the benzofuran group towards the central cavity of the receptor (Figure 7c). Nemadectin had significantly enhanced maximal level of potentiation and potency compared with ivermectin-B1a (Figure 7d,e). The longer and more rigid alkene substituent at Carbon 25 in nemadectin, together with the hydroxyl group at Carbon 23, allows for an optimal filling of the Subsite 2 space, extending spatial occupation to the region adjacent to the subsite defined by the sidechain of Glu56 (Figure 7f). This may explain the increased activity of nemadectin, although the pose also reveals the benzofuran group is pulled away from Subsite 1 and towards the central cavity similar to selamectin (Figure 7c). Eprinomectin shares the Carbon 22-23 double bond of abamectin but also an acetamide addition to the disaccharide group. However, the activity of eprinomectin is not significantly different from ivermectin-B1a (Table 1). Compound 10 has a small methoxy addition to Carbon 4 of the benzofuran group and methylation of the hydroxyl group of Carbon 4" in the disaccharide group. These additions are tolerated and the activity

14765381, 2025, 21, Downloaded from https://bpspubs.

elibrary.wiley.com/doi/10.1111/bph.70121 by University Of East Anglia, Wiley Online Library on [08/10/2025]. See the Terms

and Condition

.) on Wiley Online Library for rules of use; OA articles are governed by the applicable Creative Commons License



Impact of subtle enantiomeric changes in the spiroketal group on ivermectin analogues on pharmacological properties at the human P2X4 receptor. (a) Average trace showing effect of Compound 13 compared with ivermectin-B1a on ATP-evoked Ca<sup>2+</sup> response in 1321N1 human P2X4 cells (n = 5). (b) Compound 13 concentration–response curve showing potentiation of ATP-evoked Ca<sup>2+</sup> responses (n = 5). Average trace (c) and concentration–response curve (d) showing effect of Compound 19 on ATP-evoked  $Ca^{2+}$  responses (n = 5). The concentration-response curve to ivermectin-B1a is shown in reference as a grey curve in all test compound concentration-response curves. All  $Ca^{2+}$  responses expressed as % response to EC<sub>30</sub> ATP. Dotted lines in concentration-response curves marked ATP EC<sub>100</sub> illustrate the maximum response to ATP without test ligand. (e) Predicted binding mode of Compound 13 and Compound 19 to human P2X4 in the open channel confirmation. The two receptor subunits defining the site are represented as cyan and pink ribbons. The available binding area for Subsites 1 and 2 is represented as lilac and pink spheres, respectively. The receptor binding surface is represented as green (lipophilic) and pink (hydrophobic). Compound 13 is represented with atoms in grey, and Compound 19 with atoms in white. The structural difference between the two compounds is highlighted with a yellow circle.

of Compound 10 and ivermectin-B1a are similar (Table 1). Compounds 5, 7, 15, 17 and 18 did not significantly potentiate P2X4 responses (Table 1). When evaluating the predicted binding of these compounds, either no low-energy docking poses could be obtained, or they were found to have completely disrupted predicted binding occupying mainly the central cavity of the receptor, far from Subsite 2 and also from Subsite 1 (Figure S4c-e). These disrupted binding modes are in line with the observed lack of activity.

#### 3.6 Effect on GABA<sub>△</sub> receptors

To further the study, we investigated the structure-activity relationship of ivermectin analogues at the human GABAA receptor as ivermectin is a known modulator. We employed a mouse L (tk-) cell line with dexamethasone-inducible expression of the human GABAA  $\alpha1\beta3\gamma2$  receptor, selected as this is one of the most prevalent types of GABAA receptor found in the mammalian CNS (Feng & Forman, 2018; Fritschy & Mohler, 1995), and its activity is enhanced by ivermectin (Adelsberger et al., 2000). GABA only evoked membrane potential changes following cell treatment with dexamethasone and therefore dependent upon GABAA receptor expression (Figure 8a). GABA evoked responses with an pEC<sub>50</sub> of  $6.15 \pm 0.04$ (n = 6) (Figure 8b), which is close to the value determined by electrophysiological characterisation of the human α1β3γ2 GABA<sub>A</sub> receptor (Estrada-Mondragon & Lynch, 2015). Ivermectin-B1a directly evoked responses in the absence of GABA (Figure 8c). Ivermectin-B1a activated the GABA<sub>A</sub> receptor with an pEC<sub>50</sub> of  $5.80 \pm 0.06$  (n = 7) (Figure 8d), revealing a significantly less potent action than GABA (P < 0.01). However, the response maxima for GABA and ivermectin-B1a were not significantly different (Table 2), demonstrating that ivermectin-B1a is a full agonist at the human  $\alpha 1\beta 3\gamma 2$  GABA<sub>A</sub> receptor. Responses to ivermectin-B1a were not observed in cells not induced with dexamethasone (Figure 8e) and therefore dependent upon the expression of human  $\alpha 1\beta 3\gamma 2$  GABA<sub>A</sub> receptor. We next tested the activity of ivermectin analogues as GABAA receptor agonists using two fixed concentrations (1 and 10 µM). Approximately half of the compounds tested at 10-µM activated GABAA to >70% of

4765381, 2025, 21, Downloaded from https://bpspubs

library.wiley.com/doi/10.1111/bph.70121 by University Of East Anglia, Wiley Online Library on [08/10/2025]. See the Terms

and Conditions (https://onlinelibrary.wiley

.) on Wiley Online Library for rules of use; OA articles are governed by the applicable Creative Commons

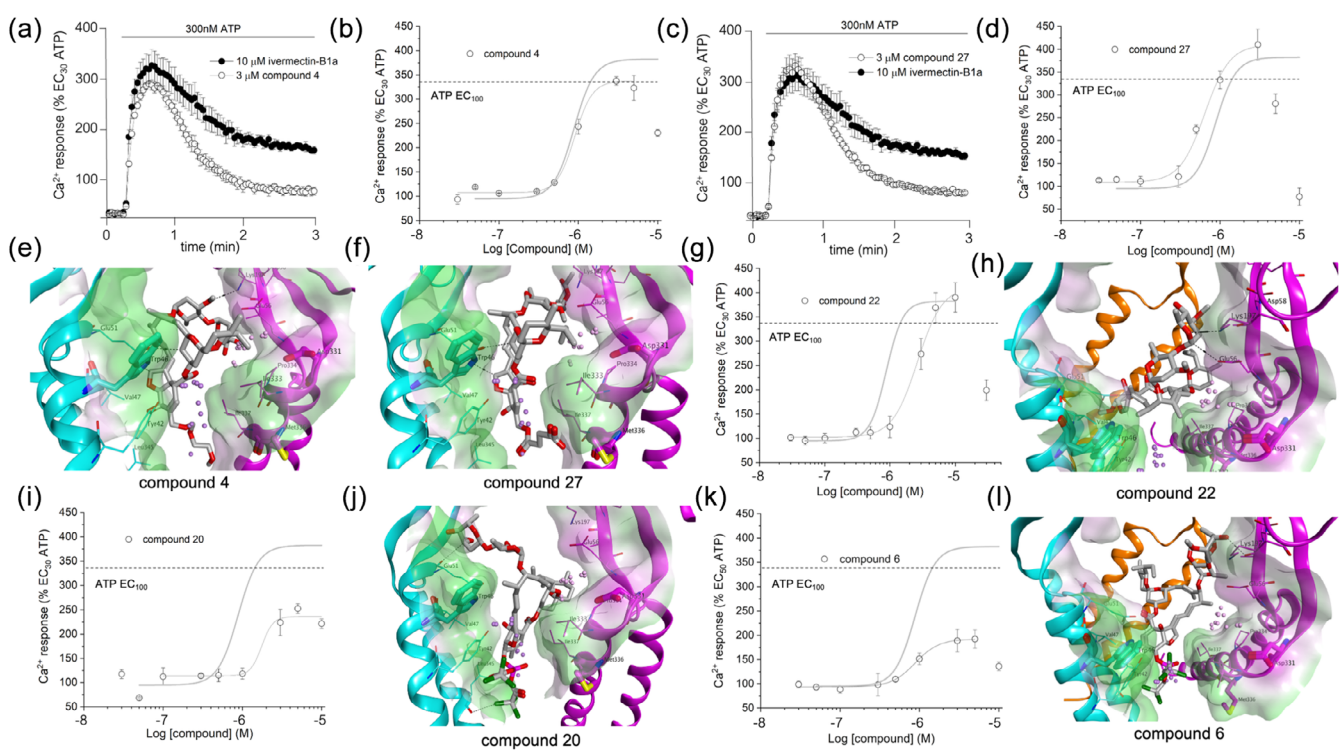


FIGURE 6 Pharmacological properties of ivermectin analogues with a modified benzofuran moiety at human P2X4. (a) Average trace showing effect of Compound 4 compared to ivermectin-B1a on ATP-evoked  $Ca^{2+}$  response in 1321N1 human P2X4 cells (n=5). (b) Compound 4 concentration-response curve showing potentiation of ATP-evoked  $Ca^{2+}$  responses (n=5). Average trace (c) and concentration-response curve (d) showing effect of Compound 27 on ATP-evoked  $Ca^{2+}$  responses (n=5). (e-f) Predicted binding poses for Compounds 4 and 27. (g) Compound 22 concentration-response curve showing potentiation of ATP-evoked  $Ca^{2+}$  responses (n=5) and (h) predicted binding pose. (i) Compound 20 concentration-response curve showing potentiation of ATP-evoked  $Ca^{2+}$  responses (n=5) and (j) predicted binding pose. (k) Compound 6 concentration-response curve showing potentiation of ATP-evoked  $Ca^{2+}$  responses (n=5) and (j) predicted binding pose. The concentration-response curve for ivermectin-B1a is shown in reference as a grey curve in all test compound concentration-response curves. All  $Ca^{2+}$  responses expressed as % response to  $EC_{30}$  ATP. For all binding predictions, the two receptor subunits defining the site are represented as cyan and pink ribbons. The available binding area for Subsites 1 and 2 is represented as lilac and pink spheres, respectively. The receptor binding surface is represented as green (lipophilic) and pink (hydrophobic). Relevant receptor residues are shown with carbon atoms coloured according to their ribbon, and ligand-receptor interactions represented as black dotted lines. Dotted lines in concentration-response curves marked ATP  $EC_{100}$  illustrate the maximum response to ATP without test ligand.

the maximal response to GABA, and approximately 20% of compounds displayed no significant activity (Figure 8f). The majority of compounds lacking activity at P2X4 receptors (Table 1) also lacked activity at GABAA receptors (Table 2). Compounds 11 and 12 lacked activity at GABAA but displayed modest activity at P2X4 (Tables 1 and 2). Nemadectin, which was more potent and more efficacious at human P2X4 compared with ivermectin-B1a (Figure 6) (Table 1), lacked activity at GABAA when tested at 1  $\mu$ M but partially activated GABAA at 10  $\mu$ M (Table 2), suggesting selectivity for P2X4 over GABAA receptors.

#### 4 | DISCUSSION

The first drug to be approved for use targeting P2X receptors is MK-7264 (Gefapixant) (Richards et al., 2019), a derivative of the anti-bacterial agent trimethoprim that inhibits dihydrofolate reductase. Ivermectin in this regard is similar, a compound modulating a different

target in a human pathogen but with activity at a human P2X receptor. Our molecular modelling studies of the ivermectin-B1a binding mode are well supported by the pharmacological properties of the ivermectin analogues tested. Our binding mode prediction of an intersubunit binding pocket between transmembrane domains is similar to that suggested for ivermectin binding to nematode glutamate-gated chloride channels (Hattori & Gouaux, 2012). Our docking of ivermectin-B1a within the allosteric pocket proposed by Pasqualetto et al. (2018) predicts ivermectin interactions with a key group of amino acid residues previously shown to be important for ivermectin action at P2X4 through mutagenesis studies. These include the critical role of Glu51 identified by Samways et al. (2012), transmembrane domain 1 residues around Trp46 and transmembrane 2 residues clustered in the 330-345 region (Jelinkova et al., 2008; Silberberg et al., 2007). For P2X receptors, significant conformational change within the transmembrane domain regions is reported to occur as receptors move from a closed to an ATP-bound open state (Li et al., 2010; Wang & Yu, 2016), leading to the opening of a gate and

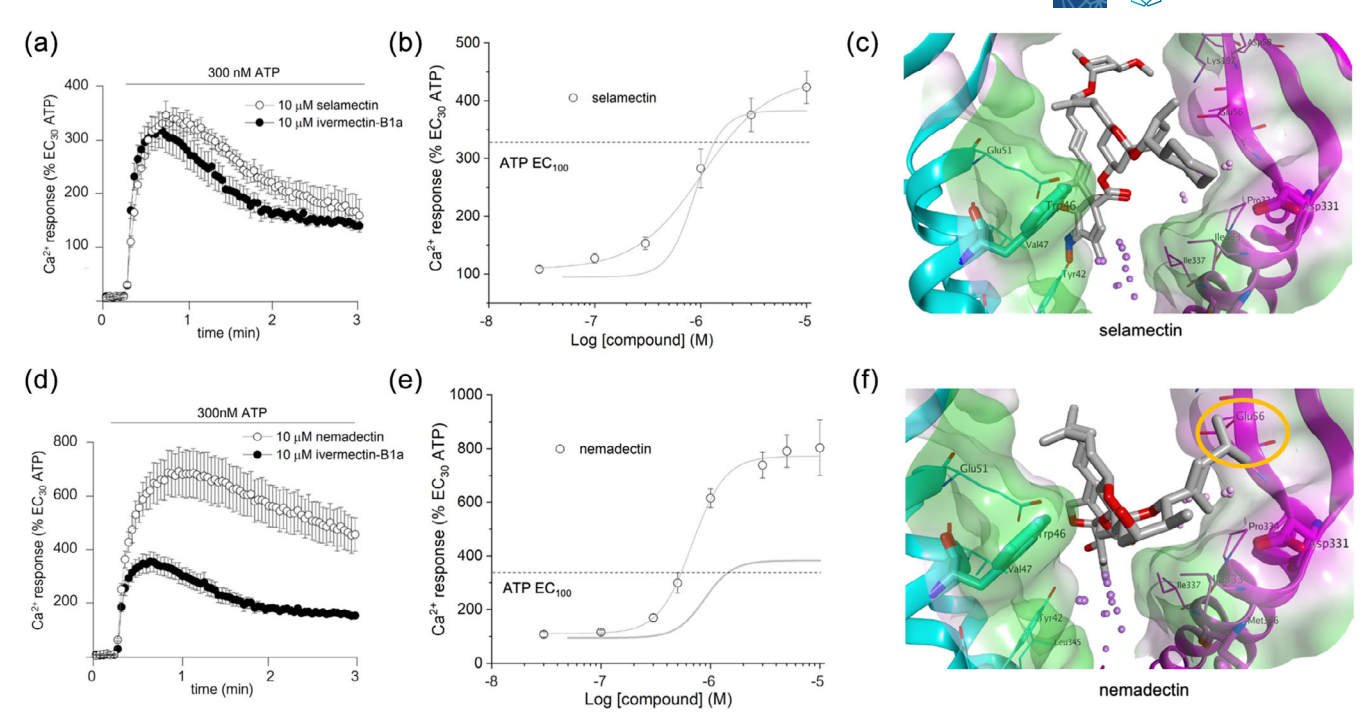


**FIGURE 7** Pharmacological properties of ivermectin analogues with mixed chemical modifications at human P2X4. (a) Average trace showing effect of selamectin compared with ivermectin-B1a on ATP-evoked  $Ca^{2+}$  response in 1321N1 human P2X4 cells (n=5). (b) Selamectin concentration-response curve showing potentiation of ATP-evoked  $Ca^{2+}$  responses (n=5). (c) Predicted binding pose for selamectin. Average trace (d) and concentration-response curve (e) showing the effect of nemadectin on ATP-evoked  $Ca^{2+}$  responses (n=5). The concentration-response curve to ivermectin-B1a is shown in reference as a grey curve in all test compound concentration-response curves. All  $Ca^{2+}$  responses expressed as % response to  $EC_{30}$  ATP. (f) Predicted binding pose for nemadectin. Additional space adjacent Subsite 2 occupied by the substituent at Carbon 25 in nemadectin is highlighted by a yellow circle. For all binding predictions, the two receptor subunits defining the site are represented as cyan and pink ribbons. The available binding area for Subsites 1 and 2 is represented as lilac and pink spheres, respectively. The receptor binding surface is represented as green (lipophilic) and pink (hydrophobic). Relevant receptor residues are shown with carbon atoms coloured according to their ribbon, and ligand-receptor interactions represented as black dotted lines. Dotted lines in concentration-response curves marked *ATP EC*<sub>100</sub> illustrate the maximum response to ATP without test ligand.

permissive ion movement. A stabilisation of this transmembrane conformation by ivermectin binding may promote stabilisation of the open channel conformation and limit movement to a desensitised channel conformation, supporting the pharmacological properties of ivermectin reported by Priel and Silberberg (2004). Hill slope coefficients for the potentiation by ivermectin analogues at P2X4 (Table 1) are >1 and therefore suggestive of positive cooperation in action of ivermectin, consistent with the original observations of Priel and Silberberg (2004). The exception was Compound 11 where the Hill slope coefficient was <1 suggesting no cooperation, though the reason for this is currently not understood. PAM interaction at Subsites 1 and 2 may serve to stabilise the transmembrane domains, holding the channel open or limiting conformational change to a desensitised state as occurs with prolonged agonist exposure (Fountain & North, 2006). Indeed, mutations close to Subsite 2 in other P2X receptor subtypes cause spontaneous channel opening (Cao et al., 2007). Previous mutagenesis supports the role of residues within Subsites 1 and 2 in mediating the effect of ivermectin on P2X4 (Silberberg et al., 2007). Amino acid residues within Subsite 2 have been proposed to mediate the inhibitory effects of ethanol on P2X4 receptors (Asatryan et al., 2010). Interestingly, the inhibitory effect of

ethanol at P2X4 is antagonised by ivermectin (Asatryan et al., 2010), supporting our predicted importance of Subsite 2 in ivermectin binding and response potentiation. The presence of an intersubunit binding site for ivermectin may also impact on the activity of ivermectin at proposed P2X4 heteromeric receptors (Harhun et al., 2014; Nicke et al., 2005).

Investigation of the pharmacological properties of ivermectin analogues allows for the identification of several trends in ligand chemistry and activity at the human P2X4 receptor. First, it is evident that the large disaccharide moiety is not required for ligand activity, having no influence on ligand potency or level of potentiation. Compounds such as milbemectin that lack the disaccharide moiety retain the potency and level of potentiation of ivermectin-B1a. Chemical additions to the terminus of the disaccharide moiety are also well tolerated, suggesting very limited spatial restraints when accommodating the disaccharide moiety when ivermectin-B1a binds to the P2X4 receptor. Our binding mode prediction of ivermectin-B1a supports no contribution of the disaccharide moiety to the pharmacological properties of ivermectin, with no predicted binding interaction between atoms of ivermectin-B1a and amino acid residues of P2X4, apart from a Lys197 nonbonded interaction. The extension of the disaccharide

5298

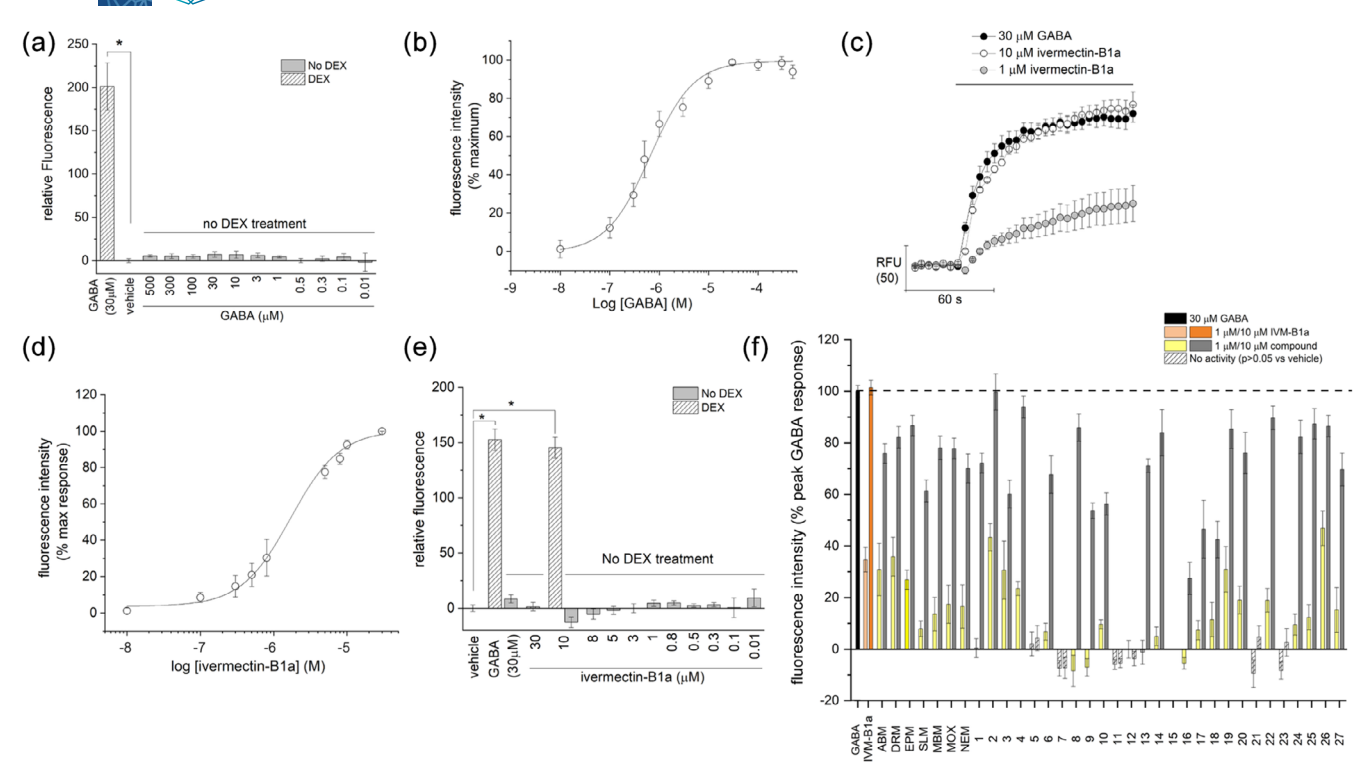


**FIGURE 8** Pharmacological properties of ivermectin analogues at the human GABA<sub>A</sub> receptor. (a) Effect of GABA on membrane potential responses in mouse L (tk-) with and without induction of human  $\alpha1\beta3\gamma2$  GABA<sub>A</sub> receptor expression with dexamethasone (DEX) treatment (n=5). (b) Concentration–response relationship of GABA in human  $\alpha1\beta3\gamma2$  GABA<sub>A</sub> receptor expressing mouse L (tk-) cells (n=5). (c) Average traces showing responses evoked by GABA and ivermectin-B1a application in human  $\alpha1\beta3\gamma2$  GABA<sub>A</sub> receptor expressing mouse L (tk-) cells (n=5). RFU is relative fluorescence units. (d) Concentration–response relationship of ivermectin-B1a in human  $\alpha1\beta3\gamma2$  GABA<sub>A</sub> receptor expressing mouse L (tk-) cells (n=5). (e) Effect of ivermectin-B1a on membrane potential responses in mouse L (tk-) with and without induction of human  $\alpha1\beta3\gamma2$  GABA<sub>A</sub> receptor expression with dexamethasone treatment (n=5). (f) Average data showing responses of GABA, ivermectin-B1a (IVM-B1a), abamectin (ABM), doramectin (DRM), eprinomectin (EPM), selamectin (SLM), milbemectin (MBM), moxidectin (MOX), nemadectin (NEM) and test Compounds 1–27, in human  $\alpha1\beta3\gamma2$  GABA<sub>A</sub> receptor expressing mouse L (tk-) cells (n=5). Responses expressed as % response 30-μM GABA. All GABA<sub>A</sub> receptor responses are assayed using a membrane potential-sensitive fluorescent dye.

moiety towards the large solvent-accessible area in the receptor central cavity also supports the lack of effective chemical modifications to the disaccharide terminus. Overall, the structure-activity analysis suggests the spiroketal moiety encompasses the most important pharmacophore elements of the ligand, as this is the region most sensitive to chemical modification. Here, hydrophobic additions are favourable for increasing potentiation of human P2X4 including cyclohexane rings and alkyl chains, increasing occupancy of Subsite 2. Enantiomeric variation in the hydrophobic ethyl group at Carbon 25 impacts accommodation of ligand at Subsite 2, as does the introduction of a Carbon 22-23 double within the spiroketal group. Compounds predicted to have very limited interaction with Subsite 2 have no activity at P2X4. This includes some chemical additions at Carbon 23, which are predicted to reduce interaction between the spiroketal group and Subsite 2. Therefore, the chemical occupation of Subsites 1 and 2 is a route to developing PAMs with greater activity at the human P2X4 receptor. In addition to these observations, several compounds tested exhibited a bell-shaped concentration-response curve. There was no apparent relationship between the chemistry of ligands tested and the molecular basis remains unclear. Several explanations for this

phenomenon are conceivable. First, as P2X4 is a desensitising receptor (Fountain & North, 2006) also known to internalise, it is possible that these properties are influenced at saturating concentrations of ligand. Second, it is possible that saturating concentrations influence binding modes or introduce negative cooperativity between multiple binding sites.

Our experiments also reveal that ivermectin-B1a can act as a full agonist at the human  $\alpha1\beta3\gamma2$  GABA<sub>A</sub> receptor, acting with equal efficacy to GABA though less potent. This is a different mode of action of ivermectin to that at P2X4, where ivermectin acts as a PAM and not as an agonist. The reported mode of action of ivermectin at GABA<sub>A</sub> receptors is variable and likely dependent upon the molecular composition of the receptor, with PAM and direct agonist effects reported (Adelsberger et al., 2000; Estrada-Mondragon & Lynch, 2015). It is not clear which mode of action of ivermectin at GABA<sub>A</sub> underlies its neurotoxic effect, but either have the potential to enhance GABAergic tone in the CNS. The ivermectin binding site in GABA<sub>A</sub> receptors has not been fully determined, though it is likely to bind at the  $\beta$ - $\gamma$  subunit interface (Estrada-Mondragon & Lynch, 2015). Endogenous neurosteroids also have an intersubunit binding site at GABA<sub>A</sub> receptors,

TABLE 2 Ivermectin analogue agonist activity at human GABA<sub>A</sub> receptors ranked by activity

Compound	Response (% GABA) <sup>a</sup>	Site(s) of chemical modification
Ivermectin-B1a	$101.42 \pm 1.65$ (10 $\mu$ M), $34.64 \pm 7.01$ (1 $\mu$ M)	_
GABA	100 (30 μΜ)	_
Compound 2	99.73 $\pm$ 7.05 (10 $\mu$ M), 43.33 $\pm$ 5.34 (1 $\mu$ M)*	Disaccharide
Compound 4	93.90 $\pm$ 4.26 (10 $\mu$ M), 23.52 $\pm$ 2.71 (1 $\mu$ M)*	Benzofuran
Compound 22	$89.68 \pm 4.53 (10 \mu\text{M})^*$ , $18.94 \pm 4.56 (1 \mu\text{M})^*$	Benzofuran
Compound 25	$87.30 \pm 5.90 (10 \mu\text{M})^*$ , $12.36 \pm 4.86 (1 \mu\text{M})^*$	Spiroketal
Eprinomectin	$86.68 \pm 3.97 (10 \mu\text{M})^*$ , $26.93 \pm 3.72 (1 \mu\text{M})^*$	Disaccharide, spiroketal
Compound 26	$86.51 \pm 4.17 (10 \mu\text{M})^*$ , $46.84 \pm 6.74 (1 \mu\text{M})^*$	Disaccharide
Compound 8	$85.90 \pm 5.27$ (10 $\mu$ M)*, no response at 1 $\mu$ M	Benzofuran
Compound 19	$85.37 \pm 7.52 (10 \mu\text{M})^*$ , $30.93 \pm 8.83 (1 \mu\text{M})^*$	Spiroketal
Compound 14	$83.96 \pm 8.93 (10 \mu\text{M})^*, 4.9 \pm 3.63 (1 \mu\text{M})^*$	Spiroketal
Compound 24	$82.30 \pm 6.50 (10 \mu\text{M})^*$ , $9.51 \pm 4.09 (1 \mu\text{M})^*$	Benzofuran
Doramectin	$82.17 \pm 4.16 (10 \mu\text{M})^*$ , $35.91 \pm 7.54 (1 \mu\text{M})^*$	Spiroketal
Milbemectin	$78.07 \pm 4.56 (10 \mu\text{M})^*$ , $13.60 \pm 6.53 (1 \mu\text{M})^*$	Disaccharide
Moxidectin	$77.85 \pm 4.56 (10 \mu\text{M})^*$ , $17.42 \pm 7.40 (1 \mu\text{M})^*$	Disaccharide, spiroketal
Compound 20	$76.08 \pm 7.99 (10 \mu\text{M})^*$ , $19.03 \pm 5.39 (1 \mu\text{M})^*$	Benzofuran
Abamectin	$75.90 \pm 3.85 (10 \mu\text{M})^*$ , $30.85 \pm 10.12 (1 \mu\text{M})^*$	Spiroketal
Compound 1	$72.14 \pm 3.84 (10 \mu\text{M})^*$ , $0.45 \pm 3.66 (1 \mu\text{M})^*$	Spiroketal
Compound 13	$71.15 \pm 2.61 (10 \mu\text{M})^*$ , no response at 1 $\mu\text{M}$	Spiroketal
Nemadectin	$70.08 \pm 5.61 (10 \mu\text{M})^*$ , $16.55 \pm 8.40 (1 \mu\text{M})^*$	Disaccharide, spiroketal
Compound 27	$69.66 \pm 6.35 (10 \mu\text{M})^*$ , $15.19 \pm 8.68 (1 \mu\text{M})^*$	Benzofuran
Compound 6	67.77 ± 7.35 (10 μM)*, 6.79 ± 3.24 (1 μM)*	Benzofuran
Selamectin	$61.35 \pm 4.25 (10 \mu\text{M})^*$ , $7.92 \pm 3.02 (1 \mu\text{M})^*$	Benzofuran, disaccharide, spirok
Compound 3	$60.12 \pm 5.38 (10 \mu\text{M})^*$ , $30.63 \pm 11.24 (1 \mu\text{M})^*$	Spiroketal
Compound 10	$56.27 \pm 4.29 (10 \mu\text{M})^*$ , $9.64 \pm 1.77 (1 \mu\text{M})^*$	Benzofuran, disaccharide
Compound 9	$53.66 \pm 3.02 (10 \mu\text{M})^*$ , no response at 1 $\mu\text{M}$	Spiroketal
Compound 17	$46.46 \pm 11.25 (10 \mu\text{M})^*$ , $7.40 \pm 3.73 (1 \mu\text{M})^*$	Benzofuran, spiroketal
Compound 18	$42.46 \pm 6.66 (10 \mu\text{M})^*$ , $11.47 \pm 6.66 (1 \mu\text{M})^*$	Benzofuran, disaccharide
Compound 16	$27.46 \pm 6.24 (10 \mu M)^*$ , no response at 1 $\mu M$	Spiroketal
Compound 21	$4.74 \pm 4.53 (10 \mu\text{M})^*$ , no response at 1 $\mu\text{M}$	Spiroketal
Compound 5	$4.30 \pm 4.84 (10 \mu\text{M})^*$ , $2.07 \pm 4.61 (1 \mu\text{M})^*$	Benzofuran, disaccharide, spirok
Compound 23	2.66 $\pm$ 5.31 (10 $\mu$ M)*, no response at 1 $\mu$ M	Spiroketal
Compound 7	No response at 1 or 10 μM	Benzofuran, disaccharide, spirok
Compound 11	No response at 1 or 10 μM	Disaccharide
Compound 12	No response at 1 or 10 μM	Spiroketal

Note: N = 8-21 for all.

though they lack agonist activity and act as PAMs (Jayakar et al., 2020). Our study focused on the  $\alpha1\beta3\gamma2$  GABA<sub>A</sub> receptor, which, along with  $\alpha1\beta2\gamma2$  GABA<sub>A</sub> (Sun et al., 2023), represents the most prevalent molecular composition of GABA<sub>A</sub> receptor in the mammalian brain (Fritschy & Mohler, 1995) and a proposed target for anti-convulsant and sedative drugs. Our study also suggests that in comparison with other anti-convulsant drugs such as benzodiazepines, which act as PAMs of GABA<sub>A</sub>, the anti-convulsant effects of

ivermectin-like molecules (Perucca et al., 2023) may be mediated through direct activation of  $\mathsf{GABA}_\mathsf{A}$ . It also remains to be determined which molecular compositions of the  $\mathsf{GABA}_\mathsf{A}$  receptor are sensitive to agonism or positive allosteric action of ivermectin-like molecules. Several compounds investigated (including Compounds 8, 11, 12 and 13) show no or very limited activity at the  $\mathsf{GABA}_\mathsf{A}$  receptor, providing an in-road to design of compounds that enhance P2X4 receptor activity with potential limited neurotoxic or other CNS adverse effects.

 $<sup>^</sup>a Response\ \%$  of 30-  $\mu M$  GABA response.

<sup>\*</sup>Denotes a significance level of P < 0.01 compared with ivermectin-B1a.

Reciprocally, some compounds (Compound 3, 9, 16 and 17) activate  $GABA_A$  but lacked P2X4 activity.

Our study reveals the concentration range over which ivermectin can increase the activity of human P2X4 and GABA<sub>A</sub> receptor activity, approximately 300 nM–10  $\mu$ M. Oral dosing of 12-mg ivermectin in human subjects results in maximum plasma concentrations of approximately 60 nM (Gonzalez-Canga et al., 2008). It is therefore unlikely that clinically approved therapeutic doses of ivermectin reach sufficient plasma levels to activation either P2X4 or GABA<sub>A</sub>. However, there is potential that this situation could change in overdose or blood–brain barrier P-glycoprotein mutations that reduce their function (Baudou et al., 2020).

In summary, this study provides novel insight into the relationship between the chemical structure of ivermectin-like molecules and their activity at human P2X4 and GABA<sub>A</sub> receptors. Combining pharmacological properties and molecular modelling, we propose a binding site for ivermectin that resides within the transmembrane domains of neighbouring subunits with two subsites that are important for the pharmacological properties of ivermectin-like molecules at the human P2X4 receptor.

#### **AUTHOR CONTRIBUTIONS**

J. L. Meades: Data curation (lead); formal analysis (equal); investigation (lead); validation (equal); writing—review and editing (supporting).

M. Bassetto: Data curation (equal); formal analysis (equal); investigation (equal); writing—review and editing (supporting).

M. C. Staiculescu: Conceptualization (supporting); project administration (supporting); resources (supporting); supervision (supporting); writing—review and editing (supporting). G. Swaminath: Conceptualization (supporting); project administration (supporting); resources (supporting); supervision (supporting); writing—review and editing (supporting). S. J. Fountain: Conceptualization (lead); formal analysis (supporting); funding acquisition (lead); methodology (supporting); project administration (equal); supervision (lead); writing—original draft (lead); writing—review and editing (equal).

#### **ACKNOWLEDGEMENTS**

This work was funded by the British Heart Foundation (PG/16/69/32194) and a Biotechnology & Biological Sciences iCASE award with Merck Sharp & Dohme LLC, a subsidiary of Merck & Co., Inc., Rahway, NJ, USA. We acknowledge Yeon-Hee Lim, Alen Northrup, Jurgen Lutz, Xiwu Chen and Vera Ares of Merck & Co., Inc., Rahway, NJ, USA, for providing the ivermectin analogues, GABAA cells, reviewing the manuscript and providing legal advice.

#### CONFLICT OF INTEREST STATEMENT

The authors declare no conflicts of interest.

#### **DATA AVAILABILITY STATEMENT**

The data that support the findings of this study are available from the corresponding author upon reasonable request, including the three-dimensional coordinates of our final model in complex with docked ivermectin-B1a.

# DECLARATION OF TRANSPARENCY AND SCIENTIFIC RIGOUR

This Declaration acknowledges that this paper adheres to the principles for transparent reporting and scientific rigour of preclinical research as stated in the BJP guidelines for Design and Analysis, and as recommended by funding agencies, publishers and other organisations engaged with supporting research.

#### ORCID

Samuel J. Fountain https://orcid.org/0000-0002-6028-0548

#### REFERENCES

Adelsberger, H., Lepier, A., & Dudel, J. (2000). Activation of rat recombinant  $\alpha 1\beta 2\gamma(2S)$  GABA(A) receptor by the insecticide ivermectin. *European Journal of Pharmacology*, 394(2–3), 163–170. https://doi.org/10.1016/S0014-2999(00)00164-3 10771281

Ahmad Nadzirin, I., Chor, A. L. T., Salleh, A. B., Rahman, M. B. A., & Tejo, B. A. (2021). Discovery of new inhibitor for the protein arginine deiminase type 4 (PAD4) by rational design of α-enolase-derived peptides. Computational Biology and Chemistry, 92, 107487. https://doi.org/10.1016/j.compbiolchem.2021.107487

Alexander, S. P., Mathie, A. A., Peters, J. A., Veale, E. L., Striessnig, J., Kelly, E., Armstrong, J. F., Faccenda, E., Harding, S. D., Davies, J. A., Aldrich, R. W., Attali, B., Baggetta, A. M., Becirovic, E., Biel, M., Bill, R. M., Caceres, A. I., Catterall, W. A., Conner, A. C., ... Zhu, M. (2023). The concise guide to PHARMACOLOGY 2023/24: Ion channels. British Journal of Pharmacology, 180, S145-S222. https://doi.org/10.1111/bph.16178

Alexander, S. P. H., Fabbro, D., Kelly, E., Mathie, A. A., Peters, J. A., Veale, E. L., Armstrong, J. F., Faccenda, E., Harding, S. D., Davies, J. A., Annett, S., Boison, D., Burns, K. E., Dessauer, C., Gertsch, J., Helsby, N. A., Izzo, A. A., Ostrom, R., Papapetropoulos, A., ... Wong, S. S. (2023). The concise guide to PHARMACOLOGY 2023/24: Enzymes. British Journal of Pharmacology, 180, S289-S373. https://doi.org/10.1111/bph.16181

Asatryan, L., Popova, M., Perkins, D., Trudell, J. R., Alkana, R. L., & Davies, D. L. (2010). Ivermectin antagonizes ethanol inhibition in purinergic P2X4 receptors. *The Journal of Pharmacology and Experimental Therapeutics*, 334(3), 720–728. https://doi.org/10.1124/jpet.110. 167908

Atack, J. R., Maubach, K. A., Wafford, K. A., O'Connor, D., Rodrigues, A. D., Evans, D. C., Tattersall, F. D., Chambers, M. S., MacLeod, A. M., Eng, W. S., & Ryan, C. (2009). *In vitro* and *in vivo* properties of 3-tert-butyl-7-(5-methylisooxazol-3-yl)-2-(1-methyl-1H-1,2,4-triazol-5-ylmethoxy)-pyrazolo[1,5-d]-[1,2,4] triazine (MRK-016), a GABAA receptor α5 subtype-selective inverse agonist. *The Journal of Pharmacology and Experimental Therapeutics*, 331(2), 470–484. https://doi.org/10.1124/jpet.109.157636

Atack, J. R., Wafford, K. A., Street, L. J., Dawson, G. R., Tye, S., Van Laere, K., Bormans, G., Sanabria-Bohórquez, S. M., Lepeleire, D. I, De Hoon, J. N., & Van Hecken, A. (2011). MRK-409 (MK-0343), a GABAA receptor subtype-selective partial agonist, is a non-sedating anxiolytic in preclinical species but causes sedation in humans. *Journal of Psychopharmacology*, 25(3), 314–328. https://doi.org/10.1177/0269881109354927

Baudou, E., Lespine, A., Durrieu, G., Francois, A., Gandia, P., Durand, C., & Cunat, S. (2020). Serious ivermectin toxicity and human *ABC1* nonsense mutations. *The New England Journal of Medicine*, *383*(8), 787–789.

Bidula, S., Nadzirin, I. B., Cominetti, M., Hickey, H., Cullum, S. A., Searcey, M., Schmid, R., & Fountain, S. J. (2022). Structural basis of the negative allosteric modulation of 5-BDBD at human P2X4 receptors.

- Molecular Pharmacology, 101(1), 33-44. https://doi.org/10.1124/molpharm.121.000402
- Burke, S. M., Avstrikova, M., Noviello, C. M., Mukhtasimova, N., Changeux, J. P., Thakur, G. A., Sine, S. M., Cecchini, M., & Hibbs, R. E. (2024). Structural mechanisms of α7 nicotinic receptor allosteric modulation and activation. *Cell*, 187(5), 1160–1176.
- Campbell, W. C. (2012). History of avermectin and ivermectin, with notes on the history of other macrocyclic lactone antiparasitic agents. *Current Pharmaceutical Biotechnology*, 13(6), 853–865. https://doi.org/10. 2174/138920112800399095
- Cao, L., Young, M. T., Broomhead, H. E., Fountain, S. J., & North, R. A. (2007). Thr339-to-serine substitution in rat P2X2 receptor second transmembrane domain causes constitutive opening and indicates a gating role for Lys308. *The Journal of Neuroscience*, 27(47), 12916–12923. https://doi.org/10.1523/JNEUROSCI.4036-07.2007
- Chandler, R. E. (2018). Serious neurological adverse events after ivermectin—Do they occur beyond the indication of onchocerciasis? The American Journal of Tropical Medicine and Hygiene, 98(2), 382–388. https://doi.org/10.4269/ajtmh.17-0042
- Coccini, T., Candura, S. M., Manzo, L., Costa, L. G., & Tonini, M. (1993). Interaction of the neurotoxic pesticides ivermectin and lindane with the enteric GABAA receptor-ionophore complex in the guinea-pig. European Journal of Pharmacology, 248(1), 1–6.
- Curtis, M. J., Alexander, S. P. H., Cortese-Krott, M., Kendall, D. A., Martemyanov, K. A., Mauro, C., Panettieri, R. A. Jr., Papapetropoulos, A., Patel, H. H., Santo, E. E., Schulz, R., Stefanska, B., Stephens, G. J., Teixeira, M. M., Vergnolle, N., Wang, X., & Ferdinandy, P. (2025). Guidance on the planning and reporting of experimental design and analysis. *Br J Pharmacol.*, 182(7), 1413–1415. https://doi.org/10.1111/bph.17441
- Dawson, G. R., Wafford, K. A., Smith, A., Marshall, G. R., Bayley, P. J., Schaeffer, J. M., Meinke, P. T., & McKernan, R. M. (2000). Anticonvulsant and adverse effects of avermectin analogs in mice are mediated through the gamma-aminobutyric acid(A) receptor. *The Journal of Pharmacology and Experimental Therapeutics*, 295(3), 1051–1060. https://doi.org/10.1016/S0022-3565(24)39005-6
- Edwards, G. (2003). Ivermectin: Does P-glycoprotein play a role in neurotoxicity? Filaria J., 2(Suppl 1), S8. https://doi.org/10.1186/1475-2883-2-S1-S8
- Estrada-Mondragon, A., & Lynch, J. W. (2015). Functional characterization of ivermectin binding sites in α1β2γ2L GABA(A) receptors. *Frontiers in Molecular Neuroscience*, 8, 55. https://doi.org/10.3389/fnmol.2015.
- Feng, H. J., & Forman, S. A. (2018). Comparison of αβδ and αβγ GABA<sub>A</sub> receptors: Allosteric modulation and identification of subunit arrangement by site-selective general anesthetics. *Pharmacological Research*, 133, 289–300. https://doi.org/10.1016/j.phrs.2017.12.031
- Fountain, S. J., & North, R. A. (2006). A C-terminal lysine that controls human P2X4 receptor desensitization. The Journal of Biological Chemistry, 281(22), 15044–15049. https://doi.org/10.1074/jbc. M600442200
- Franklin, K. M., Asatryan, L., Jakowec, M. W., Trudell, J. R., Bell, R. L., & Davies, D. L. (2014). P2X4 receptors (P2X4Rs) represent a novel target for the development of drugs to prevent and/or treat alcohol use disorders. Frontiers in Neuroscience, 8, 1–12.
- Fritschy, J. M., & Mohler, H. (1995). GABAA-receptor heterogeneity in the adult rat brain: Differential regional and cellular distribution of seven major subunits. *The Journal of Comparative Neurology*, 359(1), 154–194. https://doi.org/10.1002/cne.903590111
- Gonzalez-Canga, A., Sahagún Prieto, A. M., Diez Liébana, M. J., Fernández Martínez, N., Sierra Vega, M., & García Vieitez, J. J. (2008). The pharmacokinetics and interactions of ivermectin in humans—A mini-review. *The AAPS Journal*, 10, 42–46.
- Harhun, M. I., Povstyan, O. V., Albert, A. P., & Nichols, C. M. (2014). ATPevoked sustained vasoconstrictions mediated by heteromeric P2X1/4

- receptors in cerebral arteries. *Stroke*, 45(8), 2444–2450. https://doi.org/10.1161/STROKEAHA.114.005544
- Hattori, M., & Gouaux, E. (2012). Molecular mechanism of ATP binding and ion channel activation in P2X receptors. *Nature*, 485(7397), 207– 212. https://doi.org/10.1038/nature11010
- Hibbs, R. E., & Gouaux, E. (2011). Principles of activation and permeation in an anion-selective Cys-loop receptor. *Nature*, 474(7349), 54–60. https://doi.org/10.1038/nature10139
- Jayakar, S. S., Chiara, D. C., Zhou, X., Wu, B., Bruzik, K. S., Miller, K. W., & Cohen, J. B. (2020). Photoaffinity labeling identifies an intersubunit steroid-binding site in heteromeric GABA type A (GABA<sub>A</sub>) receptors. The Journal of Biological Chemistry, 295(33), 11495–11512. https://doi.org/10.1074/jbc.RA120.013452
- Jelinkova, I., Vavra, V., Jindrichova, M., Obsil, T., Zemkova, H. W., Zemkova, H., & Stojilkovic, S. S. (2008). Identification of P2X4 receptor transmembrane residues contributing to channel gating and interaction with ivermectin. *Pflügers Archiv*, 456, 939–950. https://doi.org/ 10.1007/s00424-008-0450-4
- Joesch, C., Guevarra, E., Parel, S. P., Bergner, A., Zbinden, P., Konrad, D., & Albrecht, H. (2008). Use of FLIPR membrane potential dyes for validation of high-throughput screening with the FLIPR and μARCS technologies: Identification of ion channel modulators acting on the GABAA receptor. *Journal of Biomolecular Screening*, 13(3), 218–228. https://doi.org/10.1177/1087057108315036
- Krůšek, J., & Zemková, H. (1994). Effect of ivermectin on γ-aminobutyric acid-induced chloride currents in mouse hippocampal embryonic neurones. European Journal of Pharmacology, 259(2), 121–128.
- Layhadi, J. A., & Fountain, S. J. (2019). ATP-evoked intracellular Ca<sup>2+</sup> responses in M-CSF differentiated human monocyte-derived macrophage are mediated by P2X4 and P2Y11 receptor activation. *International Journal of Molecular Sciences*, 20(20), 5113. https://doi.org/10.3390/ijims20205113
- Layhadi, J. A., Turner, J., Crossman, D., & Fountain, S. J. (2018). ATP evokes Ca<sup>2+</sup> responses and CXCL5 secretion via P2X 4 receptor activation in human monocyte-derived macrophages. *Journal of Immunology*, 200(3), 1159–1168. https://doi.org/10.4049/jimmunol.1700965
- Li, M., Kawate, T., Silberberg, S. D., & Swartz, K. J. (2010). Pore-opening mechanism in trimeric P2X receptor channels. *Nature Communications*, 1(4), 44. https://doi.org/10.1038/ncomms1048 20975702
- Ménez, C., Sutra, J. F., Prichard, R., & Lespine, A. (2012). Relative neuro-toxicity of ivermectin and moxidectin in Mdr1ab (-/-) mice and effects on mammalian GABA(A) channel activity. PLoS Neglected Tropical Diseases, 6(11), e1883. https://doi.org/10.1371/journal.pntd. 0001883
- Nicke, A., Kerschensteiner, D., & Soto, F. (2005). Biochemical and functional evidence for heteromeric assembly of P2X1 and P2X4 subunits. Journal of Neurochemistry, 92(4), 925–933. https://doi.org/10.1111/j.1471-4159.2004.02939.x
- Ozaki, T., Muramatsu, R., Sasai, M., Yamamoto, M., Kubota, Y., Fujinaka, T., Yoshimine, T., & Yamashita, T. (2016). The P2X4 receptor is required for neuroprotection via ischemic preconditioning. *Scientific Reports*, 6, 25893. https://doi.org/10.1038/srep25893
- Pasqualetto, G., Brancale, A., & Young, M. T. (2018). The molecular determinants of small-molecule ligand binding at P2X receptors. Frontiers in Pharmacology, 9, 58. https://doi.org/10.3389/fphar.2018.00058
- Perucca, E., Bialer, M., & White, H. S. (2023). New GABA-targeting therapies for the treatment of seizures and epilepsy: I. Role of GABA as a modulator of seizure activity and recently approved medications acting on the GABA system. CNS Drugs, 37(9), 755–779. https://doi.org/10.1007/s40263-023-01027-2
- Priel, A., & Silberberg, S. D. (2004). Mechanism of ivermectin facilitation of human P2X4 receptor channels. *The Journal of General Physiology*, 123(3), 281–293. https://doi.org/10.1085/jgp.200308986
- Richards, D., Gever, J. R., Ford, A. P., & Fountain, S. J. (2019). Action of MK-7264 (gefapixant) at human P2X3 and P2X2/3 receptors and



- in vivo efficacy in models of sensitisation. *British Journal of Pharmacology*, 176, 2279–2291. https://doi.org/10.1111/bph.14677
- Rubio, M. E., & Soto, F. (2001). Distinct localization of P2X receptors at excitatory postsynaptic specializations. The Journal of Neuroscience, 21, 641–653. https://doi.org/10.1523/JNEUROSCI.21-02-00641.2001
- Samways, D. S. K., Khakhs, B. S., & Egan, T. M. (2012). Allosteric modulation of Ca<sup>2+</sup> flux in ligand-gated cation channel (P2X4) by actions on lateral portals. *The Journal of Biological Chemistry*, 287(10), 7594–7602.
- Shan, Q., Haddrill, J. L., & Lynch, J. W. (2001). Ivermectin, an unconventional agonist of the glycine receptor chloride channel. *The Journal of Biological Chemistry*, 276(16), 12556–12564. https://doi.org/10.1074/jbc.M011264200
- Sievers, F., Wilm, A., Dineen, D., Gibson, T. J., Karplus, K., Li, W., Lopez, R., McWilliam, H., Remmert, M., Söding, J., Thompson, J. D., & Higgins, D. G. (2011). Fast, scalable generation of high-quality protein multiple sequence alignments using Clustal Omega. *Molecular Systems Biology*, 7, 539. https://doi.org/10.1038/msb.2011.75
- Silberberg, S. D., Li, M., & Swartz, K. J. (2007). Ivermectin interaction with transmembrane helices reveals widespread rearrangements during opening of P2X receptor channels. *Neuron*, *54*(2), 263–274. https://doi.org/10.1016/j.neuron.2007.03.020
- Spampanato, J., Gibson, A., & Dudek, F. E. (2018). The antihelminthic moxidectin enhances tonic GABA currents in rodent hippocampal pyramidal neurons. *Journal of Neurophysiology*, 119(5), 1693–1698. https://doi.org/10.1152/jn.00587.2017
- Stokes, L., Layhadi, J. A., Bibic, L., Dhuna, K., & Fountain, S. J. (2017). P2X4 receptor function in the nervous system and current breakthroughs in pharmacology. Frontiers in Pharmacology, 8, 291. https://doi.org/10.3389/fphar.2017.00291
- Stokes, L., Scurrah, K., Ellis, J. A., Cromer, B. A., Skarratt, K. K., Gu, B. J., Harrap, S. B., & Wiley, J. S. (2011). A loss-of-function polymorphism in the human P2X4 receptor is associated with increased pulse pressure. *Hypertension*, *58*(6), 1086–1092. https://doi.org/10.1161/HYPERTENSIONAHA.111.176180
- Sun, C., Zhu, H., Clark, S., & Gouaux, E. (2023). Cryo-EM structure reveal native GABA<sub>A</sub> receptor assemblies and pharmacology. *Nature*, 622(7981), 195–201.
- Tsuda, M., Shigemoto-Mogami, Y., Koizumi, S., Mizokoshi, A., Kohsaka, S., Salter, M. W., & Inoue, K. (2003). P2X4 receptors induced in spinal microglia gate tactile allodynia after nerve injury. *Nature*, 424, 778–783. https://doi.org/10.1038/nature01786
- Tvrdonova, V., Rokic, M. B., Stojilkovic, S. S., & Zemkova, H. (2014). Identification of functionally important residues of the rat P2X4 receptor by alanine scanning mutagenesis of the dorsal fin and left flipper domains. PLoS ONE, 9(11), e112902. https://doi.org/10.1371/journal.pone. 0112902

- Wang, J., & Yu, Y. (2016). Insights into the channel gating of P2X receptors from structures, dynamics and small molecules. *Acta Pharmacologica Sinica*, 37(1), 44–55. https://doi.org/10.1038/aps.2015.127
- Weinhausen, S., Nagel, J., Namasivayam, V., Spanier, C., Abdelrahman, A., Hanck, T., Hausmann, R., & Müller, C. E. (2022). Extracellular binding sites of positive and negative allosteric P2X4 receptor modulators. *Life Sciences*, 311(Pt A), 121143. https://doi.org/10.1016/j.lfs.2022. 121143
- Wolstenholme, A. J., & Rogers, A. T. (2005). Glutamate-gated chloride channels and the mode of action of the avermectin/milbemycin anthelmintics. *Parasitology*, 131(Suppl), S85–S95.
- Yamamoto, K., Korenaga, R., Kamiya, A., & Ando, J. (2000). Fluid shear stress activates Ca<sup>2+</sup> influx into human endothelial cells via P2X4 purinoceptors. *Circulation Research*, 87(5), 385–391. https://doi.org/10. 1161/01.RES.87.5.385
- Yamamoto, K., Sokabe, T., Matsumoto, T., Yoshimura, K., Shibata, M., Ohura, N., Fukuda, T., Sato, T., Sekine, K., Kato, S., Isshiki, M., Fujita, T., Kobayashi, M., Kawamura, K., Masuda, H., Kamiya, A., & Ando, J. (2006). Impaired flow-dependent control of vascular tone and remodeling in P2X4-deficient mice. *Nature Medicine*, 12(1), 133–137. https://doi.org/10.1038/nm1338
- Yang, R., Beqiri, D., Shen, J. B., Redden, J. M., Dodge-Kafka, K., Jacobson, K. A., & Liang, B. T. (2015). P2X4 receptor-eNOS signaling pathway in cardiac myocytes as a novel protective mechanism in heart failure. Computational and Structural Biotechnology Journal, 13, 1–7. https://doi.org/10.1016/j.csbj.2014.11.002
- Yang, T., Shen, J. B., Yang, R., Redden, J., Dodge-Kafka, K., Grady, J., Jacobson, K. A., & Liang, B. T. (2014). Novel protective role of endogenous cardiac myocyte P2X4 receptors in heart failure. Circulation. Heart Failure, 7(3), 510–518. https://doi.org/10.1161/CIRCHEARTFAILURE.113.001023

#### SUPPORTING INFORMATION

Additional supporting information can be found online in the Supporting Information section at the end of this article.

How to cite this article: Meades, J. L., Bassetto, M., Staiculescu, M. C., Swaminath, G., & Fountain, S. J. (2025). Structure–activity relationship of the allosteric effects of ivermectin at human P2X4 and GABA<sub>A</sub> receptors. *British Journal of Pharmacology*, 182(21), 5286–5302. <a href="https://doi.org/10.1111/bph.70121">https://doi.org/10.1111/bph.70121</a>